Geological Society of America
3300 Penrose Place
P.O. Box 9140
Boulder, CO 80301
(303) 447-2020 • fax 303-357-1073
www.geosociety.org

Geological Society of America
Special Paper 401
2006

Intraclast breccias in laminated sequences reviewed: Recorders of paleo-earthquakes

Amotz Agnon
Institute of Earth Sciences, The Hebrew University, Jerusalem 91904, Israel

Claudia Migowski
GeoForschungsZentrum, Climate Dynamics and Sediments, Potsdam, Telegrafenberg D-14473, Germany

Shmuel Marco
Department of Geophysics and Planetary Sciences, Tel Aviv University, Tel Aviv, 69978 Israel

ABSTRACT

Observations of intraclast breccia layers in the Dead Sea basin, formerly termed "mixed layers," provide an exceptionally long and detailed record of past earthquakes and define a frontier of paleoseismic research. Multiple studies of these seismites have advanced our understanding of the earthquake history of the Dead Sea and of the processes that form the intraclast breccias. In this paper, we describe a systematic study of intraclast breccia layers in laminated sequences.

The relationship of intraclast breccia layers to intraformational fault scarps has motivated the investigation of these seismites. Geophysical evidence shows that the faults extend into the subsurface, supporting their potential association with strong earthquakes.

We define field criteria for the recognition of intraclast breccias, focusing on features diagnostic of a seismic origin. The field criteria stem from our understanding of the mechanisms of breccia formation, which include ground acceleration, shearing, liquefaction, water escape, fluidization, and resuspension of the originally laminated mud.

Comparison between a dated record of breccia layer and the record of historical earthquakes provides an independent test for a seismic origin. The historical dating is significantly more precise and accurate than the radiocarbon dating of breccia layers. Yet, assuming that the lamination of the sediments shows an annual cycle, the precision of counting laminae may approach the precision of the historical record. A similar accuracy is then expected for the intervals between earthquakes. We review our work based on counting laminae representing the historical period, mutually corroborating the seismic origin and the annual lamination.

The correlation of documented historical earthquakes with individual breccia layers provides quantitative estimates for the threshold of ground motion for breccia formation in terms of earthquake magnitude and epicentral distance.

The investigation of breccia layers and the associated historical earthquakes has underscored cases in which a breccia layer represents a pair of earthquakes. We

Agnon, A., Migowski, C., and Marco, S., 2006, Intraclast breccias in laminated sequences reviewed: Recorders of paleo-earthquakes, *in* Enzel, Y., Agnon, A., and Stein, M., eds., New frontiers in Dead Sea paleoenvironmental research: Geological Society of America Special Paper 401, p. 195–214, doi: 10.1130/2006.2401(13).

consider the resolution of individual events in records of breccia layers. A thick breccia layer can account for multiple events, biasing the paleoseismic record. The resolution of an interseismic time interval is no better than the ratio between the thickness of a breccia layer and the rate of sedimentation.

We use revised age data for the Lisan Formation and reassess temporal clustering of earthquakes during the late Pleistocene. The variation of recurrence interval corroborates significant clustering. During periods of clustered earthquakes, of order of 1000–5000 yr, the interseismic interval becomes short, and the resolution diminishes, so the peak rate of recurrence may be underestimated.

Recurrence intervals inferred from the Dead Sea record of Holocene breccia layers do not feature the extreme variation encountered in the late Pleistocene record. Yet the Holocene record shows marked transitions between periods, each with relatively uniform recurrence interval. Two of the transitions are contemporaneous with transitions in the recurrence intervals of the Anatolian faults, implying broad-scale elastic coupling.

Keywords: earthquakes, paleoseismology, seismites, Dead Sea, clustering, homogenite.

INTRODUCTION

The young discipline of paleoseismology applies geological methods to two aspects of destructive earthquakes: geological faults as earthquake sources and the recognition of geological evidence of strong ground shaking (McCalpin, 1996; Yeats et al., 1997). Earthquake sources are studied by on-fault investigations, typically excavating trenches across and along fault traces and analyzing geomorphology controlled by the fault zone. Ground shaking studies, not necessarily conducted on fault traces, are based on analyzing liquefied sands, landslides, slumps, rock-falls, and sediments deposited in water bodies (Obermeier, 1996). Rock-falls inside caves, associated with damage and growth of speleothemes, can be dated precisely by U-Th analysis of these cave deposits (Kagan et al., 2005). Water waves generated by earthquakes (tsunami and seiche) can disrupt sedimentary structures at considerable distances from the earthquake source (Cita et al., 1996; Kastens and Cita, 1981), and lacustrine seiche waves can produce slump deposits that preserve a record of past earthquakes (Chapron et al., 1999; Siegenthaler et al., 1987). While such sediments can offer evidence for past earthquakes, the disruption might also be attributed to nonseismic processes that involve high mechanical energies (e.g., Li et al., 1996). In this paper, we present recent advances in off-fault paleoseismological studies related to our ongoing research of Dead Sea sediments.

Faulted sediments in the Dead Sea basin have long been used to locate the Sinai-Arabia plate boundary (Garfunkel et al., 1981; Neev and Emery, 1967; Zak and R. Freund, 1966) and related secondary fault traces (Agnon, 1982, 1983; Bowman, 1995; Gardosh et al., 1990) (Fig. 1). A pioneering paleoseismic study of the Jericho fault trace near the Dead Sea constrained recent activity and related surface ruptures to the historical earthquakes of 31 B.C. and 749 A.D. (Reches and Hoexter, 1981, Gardosh et al., 1990). More recent paleoseismic studies outside the Dead Sea basin have added information related to the long-term behavior (Amit et al., 2002) and its slip rate for the past two millennia (Klinger et al., 2000; Meghraoui et al., 2003; Niemi et al., 2001). A unique collaboration of archaeology, history, and geology has resolved individual slip events with considerable accuracy on the Jordan Gorge segment of the Dead Sea fault (Ellenblum et al., 1998), and further studies of offset stream channels have defined a lower bound for the long-term slip rate of 3 mm/yr (Marco et al., 2005). A variety of indicators give a similar value for the Arava Valley (Fig. 1), south of the Dead Sea (Avni et al., 2000; Klinger et al., 2000). A 2000-year-old aqueduct in Syria (350 km north of the Dead Sea) is displaced 14 m, yielding a maximum slip rate of 7 mm/yr (Meghraoui et al., 2003).

The past decade has brought a surge of paleoseismic studies in the Dead Sea basin. Active fault traces have been identified as much as 3 km away from the proposed location of the master faults (Fig. 1) (Bartov, 1999; Gluck, 2001). This corroborates earlier findings by Agnon (1982, 1983) expanded by Gardosh et al. (1990). Seismic potential of main faults was also established by studying sedimentary structures away from fault traces. Liquefied sands and convoluted beds indicative of earthquake shaking (seismites) have been reported in several locations (Bartov, 1999; Bowman et al., 2000; Enzel et al., 2000; Ken-Tor et al., 2001a). Along with these earthquake-related sedimentary structures, another kind of seismites unique to laminated sediments has been recognized: intraclast breccias (previously termed "mixed layers") that punctuate sequences of uniformly laminated late Quaternary lacustrine sediments (Marco and Agnon, 1995). Intraclast breccias formed by earthquake shaking have been reported from elsewhere (e.g., Davenport and Ringrose, 1987), and in places convincingly related to earthquakes (Doig, 1991).

Expansive outcrops of late Quaternary sediments in the Dead Sea region establish direct links between on-fault and off-fault observations. Intraclast breccias derived from laminated chalks in the Dead Sea basin are associated with surface faulting, which

provides a stratigraphic test for temporal relationships between homogenization of the laminated sediment and surface faulting (Marco and Agnon, 2005). Moreover, the Dead Sea sediments are radiometrically datable (Haase-Schramm et al., 2004; Stein and Goldstein, this volume), and independent historical evidence for earthquakes is abundant (Ambraseys et al., 1994; Amiran et al., 1994; Guidoboni, 1994). Therefore, the Dead Sea intraclast breccias hold promise for a deeper understanding of soft-sediment deformation, earthquake shaking, and the seismotectonics of the Dead Sea fault, a model continental transform (Freund, 1965; Garfunkel, 1981; Quennell, 1956; Wilson, 1965).

Spectacular examples of convoluted sediments in the laminar Lisan Formation in the Dead Sea basin have attracted the attention of sedimentologists and overshadowed the less remarkable intraclast breccias. Early works ascribed the convoluted bedding to décollement structures, implying contortion at some finite depth in the sediment (Pettijohn et al., 1987). El-Isa and Mustafa (1986) postulated that the structures formed when the deformed sedimentary layer was at the lakebed. These authors pioneered attempts to extract quantitative information on earthquake return intervals from the stratigraphic distribution of convoluted beds in a section of the Lisan Formation. Slump structures identified in a seismic reflection survey at the Jordan delta were attributed to the 1927 A.D. earthquake (Niemi and Ben-Avraham, 1994). Uncertainty regarding the burial depth of the sediment and the source of energy for deforming the soft sediments have hindered the use of these sedimentary structures to decipher the Late Quaternary seismicity in the Dead Sea.

The discovery of syndepositional faults juxtaposed to intraclast breccias in the Dead Sea basin (Marco and Agnon, 1995) created an opportunity to constrain the lake bottom conditions during homogenization of the originally laminated sediment. During the decade since the recognition of fault-related intraclast breccias, we have established a hypothesis that such layers are seismites; i.e., layers recording seismically-triggered deformation. Our investigation includes a direct correlation of intraclast breccia with synsedimentary faults, the temporal correlation with historical earthquakes, laboratory experiments, and mechanical analyses. Here we review our geological studies related to the original work and present additional results.

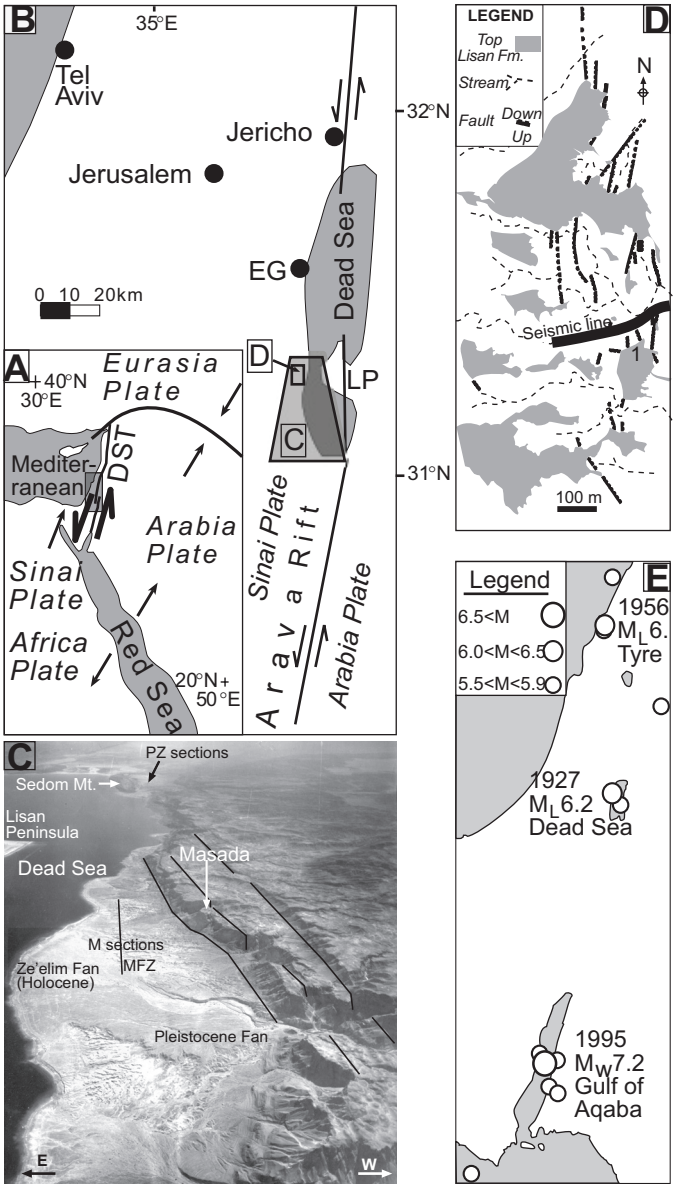

Figure 1. (A) Tectonic plates in the Middle East. The Dead Sea Transform (DST) transfers the opening at the Red Sea to the East Anatolian Fault and the Taurus-Zagros collision zone. (B) Main tectonic elements and locations of studied sections: LP—Lisan Peninsula, a type locality for the late Pleistocene Lisan Formation; EG—Ein Gedi Spa, where a continuous core of late Holocene age was recovered. (C) An oblique air photo looking southward at the southwestern part of the Dead Sea showing faults (solid lines) and locations of studied late Pleistocene sections M and PZ. MFZ—Masada Fault Zone. The photo was taken in 1940 when the lake level was 395 m below sea level. The current level is 420 m below sea level; additional area has emerged, including the Ze'elim fan outcrop. (D) Map of the MFZ—a syndepositional fault zone near Masada. The general north-south trend parallels the Dead Sea transform in the area and principal morphotectonic features to east and west of fault zone. The faults are all normal with planes striking north and a few strike northeast or southeast. Dips are between 40° and 70° eastward as well as westward. Solid line marks the location of geophysical profiles (Figs. 5–7) illuminating the fault zone in the subsurface. (E) Earthquake epicenters of M_L > 5.5 since 1900 (data from http://www.gii.co.il/html/seis/seis_fs.html; http://www.seismology.harvard.edu; Hofstetter et al., 2003).

INTRACLAST BRECCIA LAYERS

Terminology

The following terms have been used in the literature to describe various types of deformed unconsolidated sedimentary layers associated with earthquakes:

- mixed layers (Marco and Agnon, 1995; Marco et al., 1996b): this term may cause confusion with a number of unrelated uses in the earth sciences;
- mixtites (Jackson and Bates, 1997): this term describes any clastic layer regardless of composition or origin; any flood deposit may fall in this category;

- homogenites (Kastens and Cita, 1981): the term stresses uniform composition of the deposit, yet does not account for systematic variations across the layer;
- seismites (Seilacher, 1969): this term is interpretative; and
- intraclast breccias (Marco and Agnon, 2005): we use this descriptive term to separate observations from interpretations: "intraclast" refers to the origin of the clasts being reworked from within the sedimentary section (Jackson and Bates, 1997), and "breccia" refers to the texture of the deposit.

Character of Intraclast Breccias

Intraclast breccias are distinctive in sequences that are otherwise well-bedded or, better yet, laminated. Lamination is typical in the lacustrine facies of the Dead Sea deposits and makes recognition of intraclast breccias practical because of the conspicuous alternation between chemically precipitated white aragonite and darker detritus (Fig. 2) (Katz et al., 1977).

In the present context, intraclast breccias within a laminated sequence can be distinguished by the following criteria:

1. The primary mineralogical composition of an intraclast breccia is identical to the underlying strata (and typically the overlying layers also). Thus, the intraclast breccia appears similar to the enclosing deposits. The absence of fine-scale lamination observed from a short distance helps to recognize the intraclast breccia in the field.
2. Fragments of laminae may vary in distributions of size. Tabular fragments of competent laminae (with the long dimension commonly 1–5 mm) float in a fine-grained matrix. Graded bedding is common, either fining or coarsening upward.
3. Intraclast breccia layers are typically several centimeters thick, but can be as thin as a few laminae (viewed under a microscope; cf. Fig. 2B).
4. The upper contact of an intraclast breccia is invariably sharp and is typically overlain by laminated beds.
5. Basal contacts can be gradual, but occasionally are sharp. In the former case, folded and torn packets of laminae are abundant (Figs. 2A, 2C).
6. The verified lateral extent of individual intraclast breccias is on the order of 100 m. Over lateral distances of several tens of meters, the layers vary little in thickness, except where they onlap local paleorelief that formed during earthquakes (Fig. 3).

Jones and Omoto (2000) suggest the following criteria for the identification of seismic triggering of soft sediment deformation: (1) geological setting, (2) extent of the deformed units, (3) absence of evidence indicating other potential trigger mechanisms, and (4) presence of evidence of other potential trigger mechanisms elsewhere in the stratigraphic section associated with undeformed sediment. Intraclast breccia layers in the sediments studied satisfy all these criteria.

Other Reports of Seismites and Intraclast Breccias

The Dead Sea intraclast breccias have many similarities to seismites described from the lacustrine environment as well as from glacial deposits and volcanic terrains. Breccia layers associated with microfaults and intraformational folds in glacial deposits were reported in Scotland (Davenport and Ringrose, 1987). Earthquake-induced soft sediment deformation in Late Pleistocene lacustrine beds associated with activity at the Narugo Volcano, Japan, has been reported by Jones and Omoto (2000), who suggest the above-mentioned criteria to identify seismic triggering agents.

Most of the paleoseismic studies focus on Pleistocene to Recent deposits, but seismites have been reported in significantly older rocks, including Silurian strata (Kahle, 2002) and laminated Neogene deposits in Spain (Rodríguez-Pascua et al., 2003). In the area of the Dead Sea Rift, intraclast breccia layers are also present in Senonian chert (Mishash Formation), which crops out near the Lisan Formation (Fig. 2B). Similar fabrics in the breccias in these formations prompted Kolodny et al. (2005) to suggest a similar mechanism of formation.

Interpreting the origin of ancient seismites often relies on intuition and on understanding models of the mechanism of their formation. Features interpreted as ancient seismites should resemble those formed by modern earthquake deformation. Soft sediment deformation associated with strong earthquakes is documented by observations of recent seismic events (Allen, 1974; Sims, 1973). Earthquakes have caused silting and resuspension of sediments in Canadian lakes in association with earthquakes and in turbid water observed in lakes <10 km from the epicenter of the 1935 Témiskaming, Canada, M 6.3 earthquake (Doig, 1990, 1991). Piston cores from the bottom of that lake recovered a 20-cm-thick chaotic layer composed of tabular fragments derived from a preexisting silt layer. Graded bedding has been suggested as a criterion for subaqueous liquefaction based on observations in Kobe, Japan, following the 1995 earthquake (Kitamura et al., 2002).

Earthquake-induced historical homogenites are reported in Lake Lucerne, Switzerland (Siegenthaler et al., 1987). Lake Le Bourget, France, has homogenites that correlate with the A.D. 1822 earthquake (local intensity VII–VIII), the strongest known historical earthquake of the French outer Alps (Chapron et al., 1999). Historical accounts of this earthquake report violent lake water oscillations, which were probably a seiche, and an earthquake-induced subaqueous slide may have formed the homogenite layer.

The Formation of Intraclast Breccias

The formation of intraclast breccias involves five stages (Fig. 3). First, layered deposits at the lakebed (Fig. 3A) are disrupted and deformed by ground shaking, motion of the water column, and water escape from the underlying uncompacted sediment (Fig. 3B). During this stage, the pressure of pore fluids in the sediment exceeds the confining pressure of the overlying lake

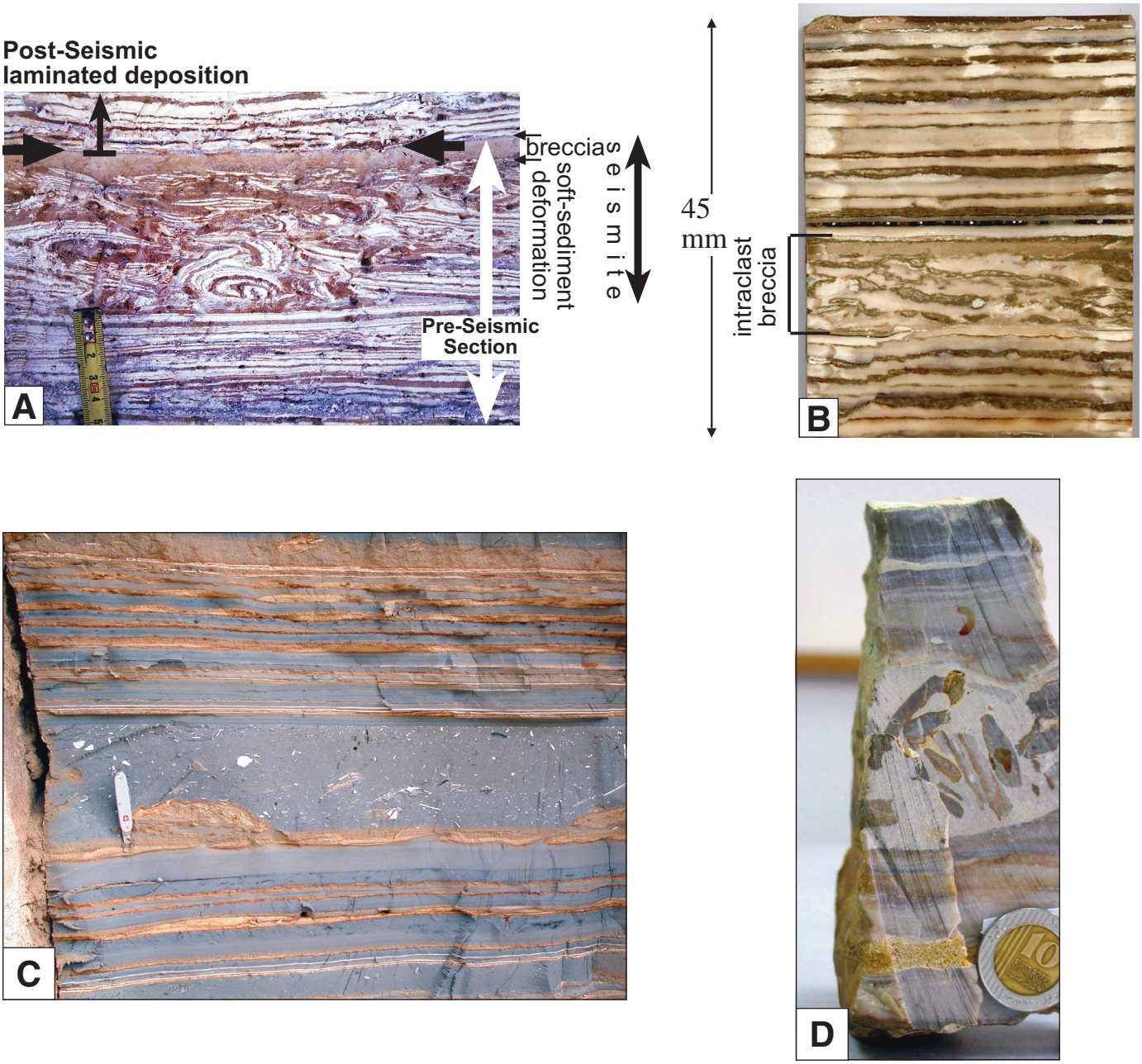

Figure 2. Selected photos of intraclast breccias. (A) Elements of a typical intraclast breccia layer overlying a disrupted sequence. (B) A micrograph of a section from the Ein Gedi core. The lowest centimeter displays an undisturbed sequence consisting of six cycles of alternating detritus and aragonite. On top of this sequence, a 1-cm-thick intraclast breccia layer comprises torn laminae of aragonite as well as detritus, topped with a millimeter of fine breccia with mixed components. The intraclast breccia layer is topped in turn by twelve cycles of alternating detritus and aragonite. (C) An intraclast breccia layer identified with the 31 B.C. earthquake (Ken-Tor et al., 2001a, 2001b). (D) An intraclast breccia from Campanian chert, near the Dead Sea rift (photo by Y. Kolodny). Kolodny et al. (2005) point out to the similarity in texture with Lisan Formation breccias and suggest a similar mechanism of formation.

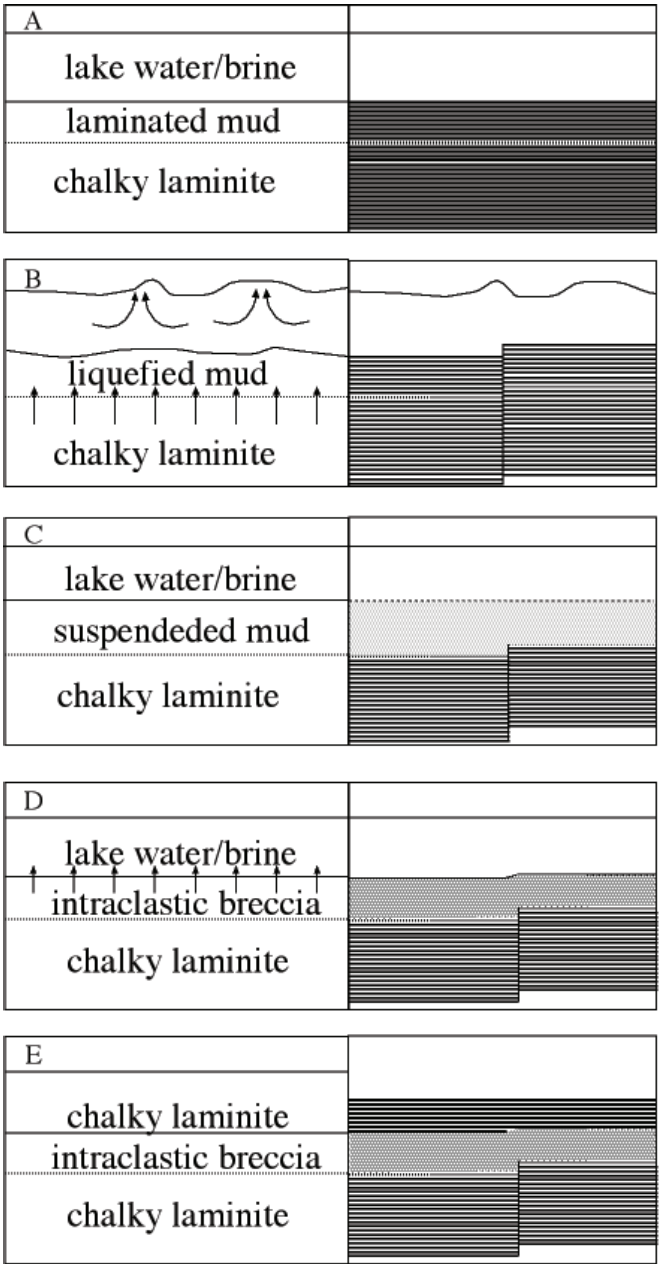

Figure 3. Schematic stages in the formation of an intraclast breccia. (A) Laminated mud is deposited over an older compact laminite. (B) Earthquake causes ground shaking, excess fluid pressure, and water waves. A fault rupture creates a topographic step at the bottom of the lake. (C) The top layers of the sediment are disrupted, laminae are torn, and the liquefied mass is suspended into the lake. (D) The suspended mud settles and forms a layer that partly fills the local relief. (E) Continual deposition covers the intraclast breccia and the residual topography with laminites.

brine, resulting in liquefaction of the sediment. Subsequently, the top of the sedimentary succession becomes fluidized and suspended at the bottom of the water body; fault ruptures can create topographic steps at the lake bottom (Fig. 3C). Seismic waves can trigger mechanical instability in the sediment, expelling pore fluid into the overlying suspension (Hamiel, 1999; Heifetz et al., 2005). Long water waves that oscillate the entire lake (seiche) carry significant momentum at the bottom of the lake, keeping the sediment suspended. After the waves have dispersed and attenuated, an intraclast breccia is deposited from the suspension by grain settling and water escape (Fig. 3D). After settling, the intraclast breccia is capped by the continuing deposition of laminated sediments that gradually bury any fault-related topography (Fig. 3E).

The intraclast breccia's texture attests to the interplay between forces in the sediment; namely, the pressure of the pore fluids, the contact forces between solid particles, and gravity. The clasts were originally part of laminae, and rupture of the laminae is a precursor of a liquefied state, where pore pressure exceeds cohesive forces and drives cracks through the sediment. As long as the pore pressure exceeds the lake pressure head, fluids that escape the liquefied bed exert drag stress on particles in the top part of the layer. When this drag exceeds gravitational forces, particles are suspended and the sediment is fluidized.

The formation energy of seismites in general is supplied by seismic shaking, but gravitational energy contributes on slopes, where the disturbed bed slides downhill, expending potential energy. Gravitational energy can also contribute to the formation of seismites where the density profile of the undisturbed sediment is inverted (dense on top): overturning the sediment releases the gravitational potential for overcoming resistance. There is no evidence that gravitational energy was a factor in the formation of common Dead Sea intraclast breccias. The seismites were deposited on flat surfaces, and no evidence for density inversion was found. Some gravitational energy is involved when pore fluid is injected upward, but most of the formation energy is of seismic origin. Three agents of seismic energy for disruption can be considered: the shaking of the ground below, the motion of the water above, and the injection of pore water from below.

Fragments of laminae in upward-fining intraclast breccias indicate that the lake-bottom sediment was compacted and cohesive before the earthquake. During the event, laminae shattered, and fragments were suspended into the fluid. Liquefaction of sediments under earthquake shaking is well documented and is traditionally related to the passage of shear waves (e.g., Allen, 1982). Yet observations of liquefaction features from recent large earthquakes highlight the role of P-waves (Lin, 1997), and engineering design based on resistance to cyclic shear loading has occasionally failed (Hatanaka et al., 1997). Observations of intraclast breccias in the Dead Sea basin have stimulated new theoretical and experimental studies of liquefaction (Bachrach et al., 2001; Hamiel, 1999; Lioubashevski et al., 1996).

An alternative mechanism is the Kelvin-Helmholtz Instability (KHI) mechanism, in which stably stratified layers undergo a shear instability during relative sliding, which is set off by

earthquake shaking (Heifetz et al., 2005). Analysis suggests a threshold for ground acceleration increasing with the thickness of the folded layers. The maximum thickness of folded layers, on the order of decimeters, corresponds to ground accelerations of up to 1 g. The application of the KHI model to earthquakes is based on a translation of the instrumentally measurable ground accelerations to pressure gradients. The KHI model is at a preliminary stage and does not provide precise correspondence between field observations and the actual driving ground accelerations. Moreover, it does not rule out alternative sources for pressure gradients, such as surface and internal waves in the depositing water body. Since water depth of Lake Lisan above the investigated area was several tens of meters (Bartov et al., 2002), ground acceleration waves might have dominated over water waves.

Association with Intraformational Faults

Several authors have cited criteria to distinguish between the seismic and nonseismic origin of soft sediment deformation features (for reviews, see Jones and Omoto, 2000; Obermeier, 1996). Marco and Agnon's (1995) studies of seismites were originally motivated by intraclast breccias juxtaposed to intraformational faults in the vicinity of Masada (Fig. 1), where a terrace capped by laminated sediments is present between the Dead Sea and the western fault escarpment (Agnon, 1983; Sagy et al., 2003). Similar exposures of fault zones juxtaposed to intraclast breccias are also present in the Lisan Peninsula. Analysis of the microstratigraphy at these sites shows simultaneity between two processes acting at the lake bottom; namely, faulting and homogenization of the lake bed (Marco and Agnon, 1995, 2005). The time interval between intraclast breccia formation and lake bottom faulting is shorter than the time it took to deposit a lamina, which is likely less than one year (see evidence below for varve-like lamination). This association is perhaps the strongest evidence for attributing datable sedimentary structures to earthquakes, hence naming them seismites. The geological observation that deformation occurred at the water-sediment interface makes intraclast breccias excellent markers to determine the times of past earthquakes, if the time of sedimentation can be determined.

The Subsurface Masada Fault Zone

The Masada fault zone has repeatedly ruptured the surface along several km (Fig. 1). In order to examine the subsurface continuity of the faults, Marco et al. (1996a) carried out ground penetrating radar (GPR) and high-resolution seismic reflection surveys to image the fault zone (Figs. 4–7).

The 275-m-long GPR survey shows fault planes extending several meters below the surface (Fig. 5). A parallel calibration profile runs at the top surface of the Lisan Formation above a buried fault whose location and dip are known from exposures (Fig. 4).

The 450-m-long seismic reflection line across the Masada fault zone overlaps the GPR profile but extends farther east and west (Fig. 6). In addition to conventional reflection data, we present diffraction data analyzed using the method proposed by Landa et al. (1987) and Kanasewich and Phadke (1988). The diffracted waves are sensitive to the discontinuities in beds due to faulting, providing an independent support for the interpretation of the reflection profile.

Three zones of discontinuous reflectors on the processed profile represent faults that extend from <0.05 s down to 0.25 s (two-way traveltime [TWTT]) at shot points 50–60, 80–95, and 125–135. The faults are also the sources of diffractions that are shown in the diffraction section from 0.05 s to 0.15 s (TWTT) at shot points ~60, 95, and 125–135 (Fig. 6).

The coincidence of the faults in the geological, radar, and seismic reflection sections shows that every outcropping fault can be traced down to ~250–300 m (Fig. 7). Eyal et al. (2002) reported similar results in another study of a fault zone in an alluvial fan . Several faults evident in the seismic section are not expressed in outcrops, which may be evidence for syndepositional faulting, or alternatively, with faults that did not rupture the surface.

Shaking Intensity Required to Brecciate Sediments

Based on correlations with historical earthquakes, Migowski et al. (2004) concluded that local intensity is a critical factor in the formation of intraclast breccia layers. We review this work below and define the conditions required to form intraclast breccias.

The Dead Sea region has not experienced strong earthquakes during the instrumentally recorded twentieth century (Fig. 1). Therefore, to assess the intensity required to brecciate laminated

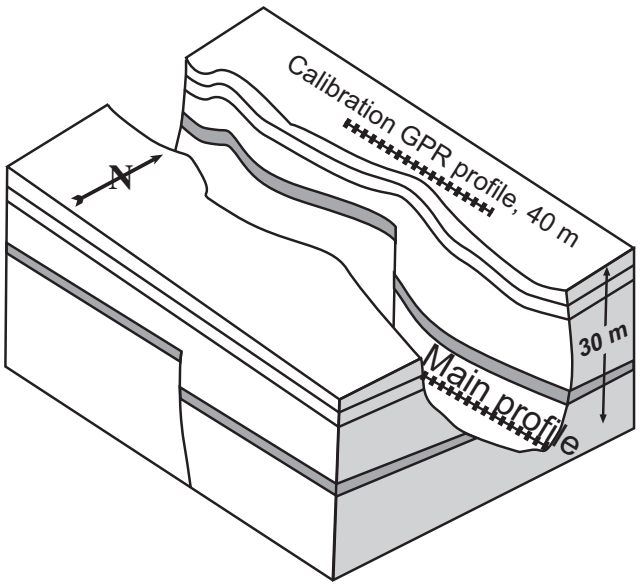

Figure 4. A schematic representation of the setting of the ground penetrating radar and seismic experiments. The 40-m-long calibration line was designed to show the pattern of the GPR image of a fault whose location is known.

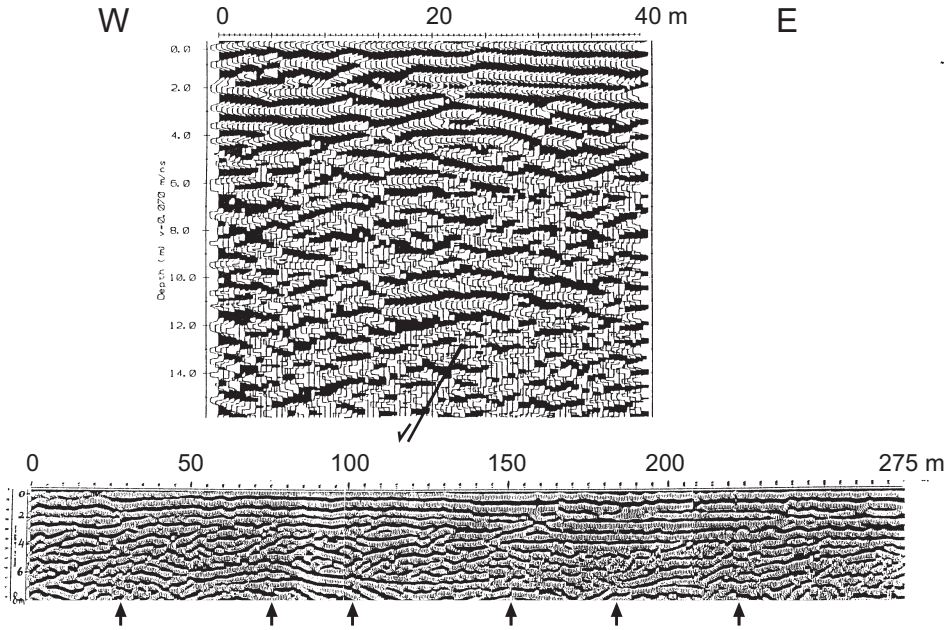

Figure 5. Top: Ground penetrating radar image of a fault buried underneath unfaulted lake Lisan deposits. Parabolic reflections are interpreted as a diffraction pattern caused by the buried fault scarp. Bottom: GPR image across the Masada fault zone. Arrows point at interpreted faults. The uppermost two "reflectors" are a direct air-wave and a surface wave.

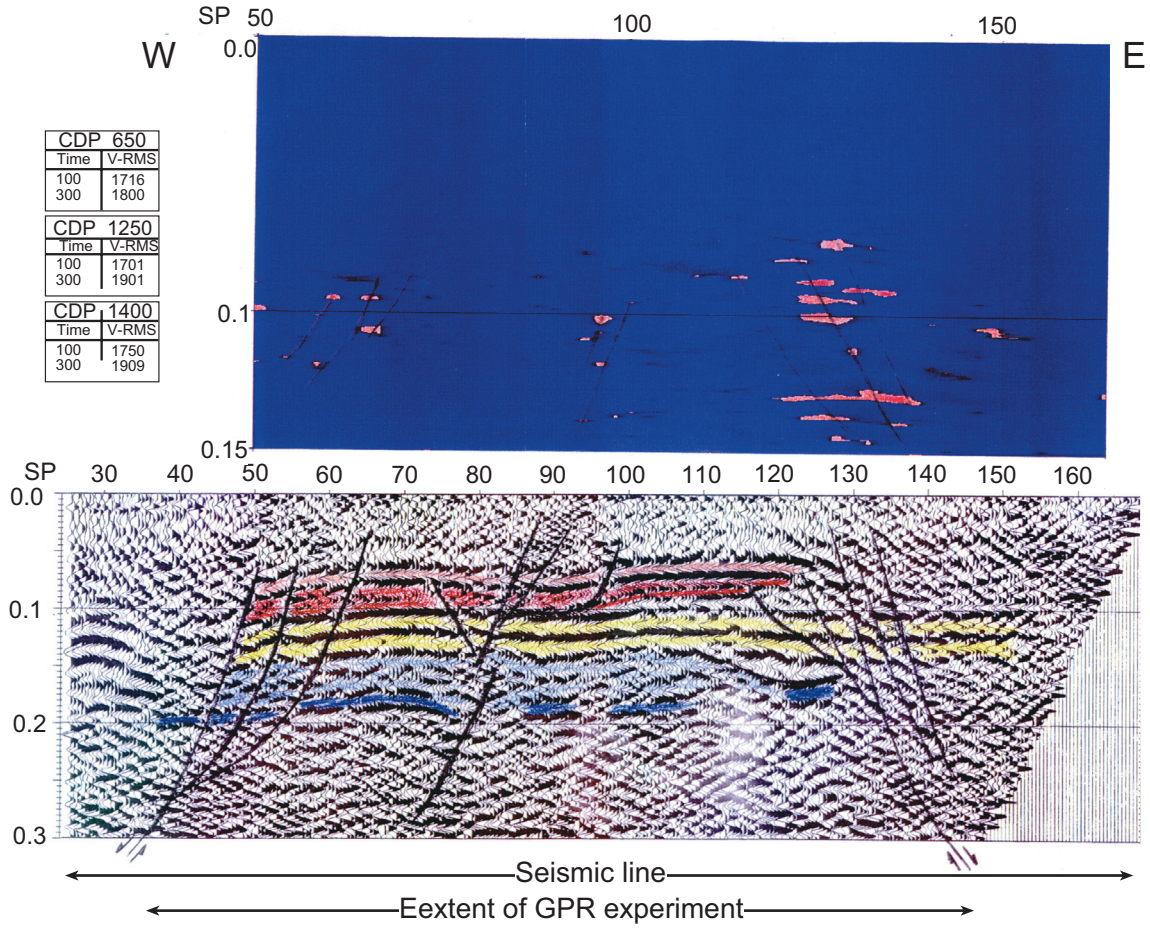

Figure 6. Results of high-resolution seismic reflection across the Masada Fault Zone revealing fault planes extending ~250 m below the surface. Source interval is 5 m; off-end cable spread with 48 channels; 10 Hz single geophones spaced at 2.5 m intervals (Marco et al., 1996a). Top: A stacked diffraction section showing three major diffraction sources (light color) from 0.05 s to 0.15 s (two-way traveltime [twtt]) at shot points ~60, 95, and 125–135. Bottom: A stacked reflection section showing three zones of discontinuous reflectors from <0.05 s down to 0.25 s (twtt) at shot points 50–60, 80–95, and 125–135. Clear reflectors are seen down to 0.2 s (twtt). Below 0.2 s, the reflection is somewhat blurred although reflector traces can be seen even at 0.3 s. Assuming a mean velocity of ~1800 m/s indicates that the faults continue down to at least 270 m (after Marco et al., 1996a).

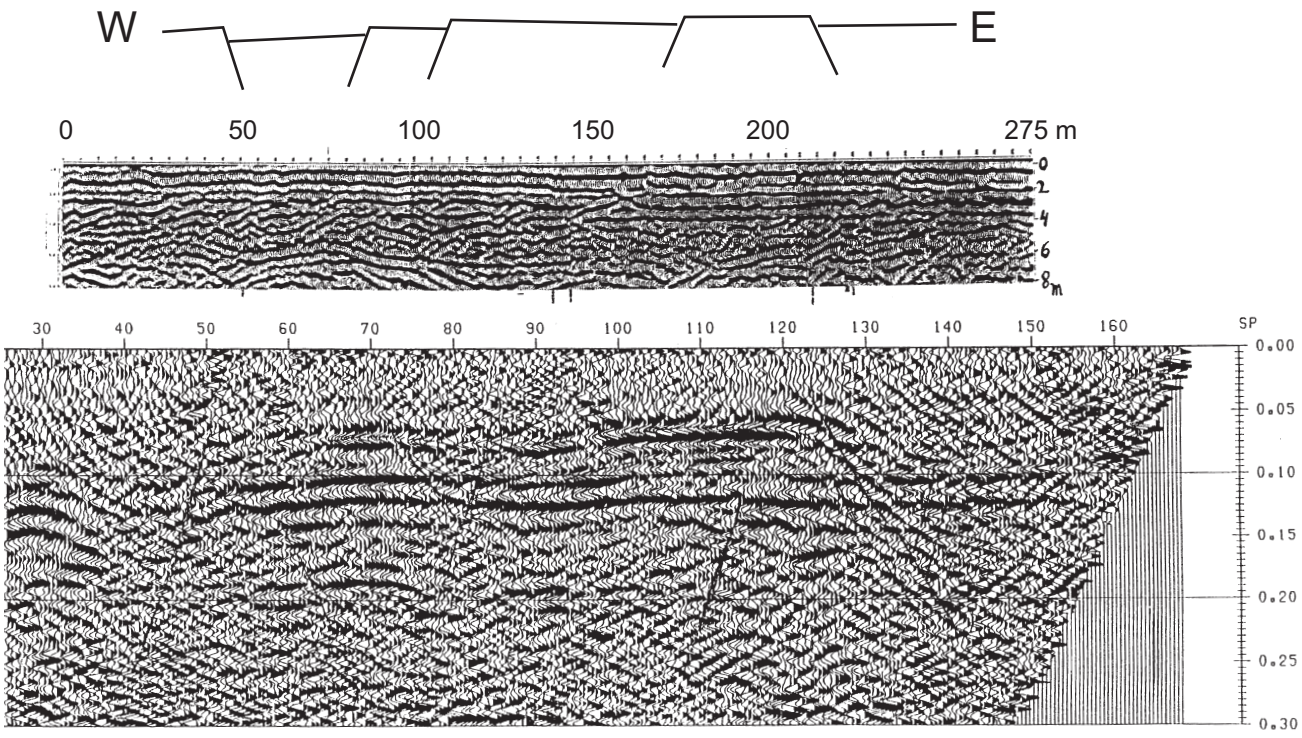

Figure 7. Geophysical imaging versus observed outcrop: Exposed section, ground penetrating radar, and seismic profiles are aligned to show the fault geometry down to ~250 m. All the exposed faults are underlain by discontinuities in GPR and seismic reflectors. However, several discontinuities are seen only at depth and are overlain by continuous reflectors. The combined image indicates that the faults are clear below the base of the Lisan Formation and are therefore interpreted as tectonic. Faults that are overlain by continuous reflectors may be interpreted as either preceding the deposition of the sequence or ruptures that did not reach the surface.

sediments, we must rely on historical records of earthquakes. The Dead Sea region has a long, rich record of historical earthquakes, which consists of information on shaking in settlements nearby (Ambraseys et al., 1994; Amiran et al., 1994; Guidoboni, 1994). Recent retreat of the Dead Sea shorelines has exposed sediments deposited in the past millennia, where the effects of known historical earthquakes can be seen in the sediments. Exposures revealing historical deposits are limited to where the lake level was higher than the level during the past decade. Even for these intervals, the sediments may lack fine bedding or may have been eroded during times of low water levels. Drill cores in lacustrine laminated facies overcome these limitations.

Another analysis, which considers both the thickness of the breccia beds and the lithology of beds directly overlying them, is applied in order to identify the stronger ($\mathbf{M} > 7$) earthquakes within the record recovered from the Lisan Formation (Begin et al., 2005). The analysis is based on the occurrence of gypsum immediately above 11 breccia layers between 54 and 16 ka, a coincidence that is explained by the triggering of a strong seiche, which mixed the stratified waters of Lake Lisan. Mixing of the sulfate-rich upper water layer with the calcium-rich lower water layer could trigger the deposition of gypsum (Stein et al., 1997a). The resulting time series of earthquakes recurrence interval is similar to the $\mathbf{M} \geq 7.2$ recurrence interval in the Dead Sea basin, as extrapolated from present seismicity; therefore, Begin et al. (2005) suggest that the present seismic regime in the Dead Sea basin, as reflected in its magnitude-frequency relationship, has been stationary for the past ~40 k.y.

EXPOSURES OF INTRACLAST BRECCIAS CAUSED BY HISTORICAL EARTHQUAKES

Ken-Tor et al. (2001a) studied Holocene outcrops of Dead Sea sediments in Ze'elim fan, east of Masada (Fig. 1), where eight late Holocene seismites are exposed due to the accelerated recess of the Dead Sea during the past decades (Fig. 8). Six intraclast breccia layers (A–F) are identified in the lacustrine laminated facies. The uppermost part of the section exposes only the near-shore sandy facies, showing two liquefied sand units (G and H). Some intraclast breccias in the lower section grade laterally into liquefied beds showing flame structures as these beds change facies into beach sands. Twenty-four radiocarbon ages of plant debris are largely consistent with the stratigraphic order in the section sampled. Ken-Tor et al. (2001a) were able to fit a model of moderately varying deposition rates (3–9 mm/yr) between hiatuses by assuming that all intraclast breccias were formed during

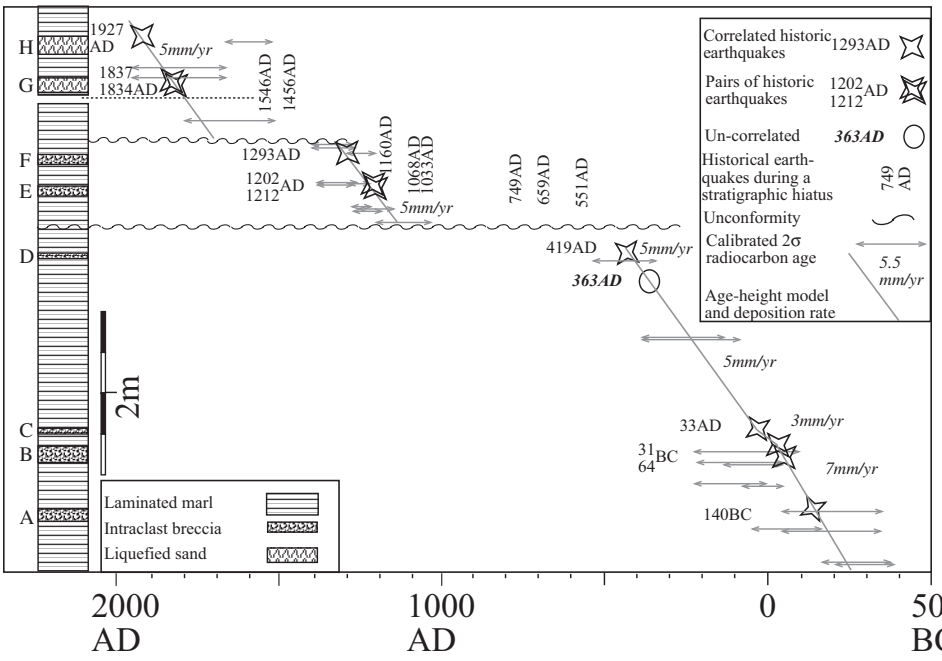

Figure 8. A modified age model for Ze'elim section studied in outcrop (Ken-Tor et al., 2001a) and drill core (Migowski et al., 2004). A–H denote events discussed in the text. The present model was constrained by two rules: (1) each event horizon (top of each intraclast breccia) matches a historical earthquake of notice, and (2) each continuous deposition segment shows a uniform deposition rate. Two outcomes support the model: Two of the breccia layers match pairs of earthquakes (64–31 B.C.; 1202–1210 A.D.) such that the earlier event horizon is within the breccia layer and the later event matches the top. With these assignments for the event horizons, the model gives a uniform rate of sedimentation of 0.5 cm/yr during the three periods separated by hiatuses.

historically recorded earthquakes (Fig. 8). Significant uncertainty remained only regarding event D (~4 m above the base of the section, Fig. 8) that could correspond to either of two historical earthquakes: 363 or 419 A.D. Ken-Tor et al. (2001a) have considered both events (compare their Figures 3 and 4).

By combining radiocarbon dating with the precise dates of historical earthquakes and with field evidence suggesting subaerial exposures, Ken-Tor et al. (2001a) determined that two unconformities exist in the section between 400 (or 420) and 1200 A.D., and between 1300 and 1750 A.D. (Fig. 9). This interpretation is remarkable in that the eight major historical earthquakes that are missing from the Ze'elim fan section have all happened during the hiatuses thus dated (551, 559, 749, 1033, 1068 1160, 1456, 1546 A.D.). This suggests that the Ze'elim earthquake record is complete for the periods of deposition, with the exception of either 363 or 419 A.D., for which only a single intraclast breccia is found. We return to this dilemma after reanalyzing the outcrop data, and again after presenting the results from drill cores.

Subsequently, Ken-Tor et al. (2001b) used the historical earthquakes to refine calibration of their radiocarbon dates and to infer that the time between death of the plant and burial in the sediment is 50 yr or less.

Figure 8 offers a revised correlation scheme between the Ze'elim stratigraphic record and the historical earthquake record that satisfies two conditions:

1. All model dates match event horizons with historical earthquakes.
2. A uniform sedimentation rate between successive event horizons and a slowly varying sedimentation rate between hiatuses. This allows interpolation between event horizons and determination of ages based on historical dates exceeding the precision of radiocarbon.

We used 24 calibrated radiocarbon ages (Bookman et al., 2004; Ken-Tor et al., 2001a) to guide the matching of the sediment height-age model. Nineteen ages are compatible with the model in that the higher bound on the age is older than the model age. For most cases, the model line goes through the calibrated age range. Five calibrated ages are younger than the model by several decades. Some incongruence can be resolved by considering low-probability ranges in the calibrated date distributions. Discrepancy may also result from sampling of roots debris that might have deteriorated in situ. Alternatively, our uniform deposition rate may be an oversimplification for this arid climate featuring irregular flash floods.

Our model indicates a strikingly uniform mean sedimentation rate during the three periods of continuous sedimentation: 5–6 mm/yr. Where data is ample, we note that the deposition rate may fluctuate by 50% around that mean rate: at the short period before the Christian era (between the events of 140 and 31 B.C.), we see an anomalously high rate of deposition (7 mm/yr). Subsequently, between 31 B.C. and 33 A.D., the rate declines to 3 mm/yr, maintaining an average of ~5 mm/yr.

This uniform deposition rate model results in breccia layer A in the section of Ken-Tor et al. (2001a) correlating with the 140 B.C. earthquake. The 64 B.C. earthquake, which was originally correlated with breccia layer A, cannot be distinguished from the 31 B.C. breccia layer. We prefer this correlation to the correlation of breccia layer A with the 64 B.C. earthquake because the latter correlation implies an excessive deposition rate of 24 mm/yr.

Our model correlates breccia layer D with the 419 A.D. earthquake, noting that this results in the 363 A.D. earthquake

being uncorrelated. Our reconstruction agrees with lamina counting data (Migowski et al., 2004) reviewed in the next section.

Historical Earthquakes and Intraclast Breccias in Drill Cores

Continuous cores from three sites along the Dead Sea shore were drilled during the fall of 1997 (Migowski et al., 2004), including cores from Ze'elim fan and Ein Gedi Spa (Fig. 1). The staggered-pair drilling technique recovered a continuous record of the subsurface sediments. We chose the Ze'elim fan site to correlate subsurface strata with the outcrops (Ken-Tor et al., 2001a, 2001b) and verify that both surface and drill core methods agree. The two other boreholes were drilled very close to the contemporary shoreline to avoid hiatuses due to lake level drops beyond the current level (Bookman et al., 2004) and to obtain data from very recent sediments. The 20-m-long Ein-Gedi core provides a continuous sedimentation record that spans the past 10,000 yr (Migowski et al., 2004). Above a 10 ka salt layer, the core contains two alternating principal facies: laminated fine-grained chalk (laminites) and bedded to massive silt. The laminated chalk contains aragonite laminae, resembling the lacustrine facies of Lisan Formation (Bartov et al., this volume).

The Ein Gedi core has penetrated 53 deformed intervals (Migowski et al., 2004, their Table 2). Many of the 53 deformed intervals in the core resemble the intraclast breccia beds of Marco and Agnon (1995). Migowski et al. (2004) focused on a 2.25-m-long interval of aragonite-rich laminites for a detailed inspection under an optical microscope. They counted couplets of detritus and chemically precipitated laminae as single depositional cycles. In some cycles, laminae of gypsum added to form triplets. They identified 1500 deposition cycles and suggested that a cycle represented one year of sedimentation. One way to test the annual depositional cycle hypothesis is to evaluate the lamina chronology with intraclast breccia events to see whether the time intervals match the historical record. Within that microscopically analyzed interval, Migowski et al. (2004) found 22 intraclast breccia layers and developed a chronological model for the sequence in which each cycle represents one year.

Migowski et al. (2004) constrained their chronological model to minimize the number of breccia beds for which no historical earthquake is known and found only one model that matched as many as 20 out of 22 breccia layers with historical earthquakes since ca. 150 B.C. (e.g., Fig. 10). They found that four additional earthquakes correspond to periods in which the record was destroyed by brecciation associated with subsequent earthquakes, postdating the missing events by several years (and, in a single case, by 33 yr). Figure 10 shows a unique situation where the contact between two breccia layers is preserved, so two earthquakes separated by 10 yr may be resolved.

The chosen matching, leaving out two subcentimeter breccia layers at 90 A.D. and 175 A.D., is significantly better than any other chronology model. The chosen model also minimizes the number of historical earthquakes for which no disturbance is shown in the sediment: six historical earthquakes from the entire

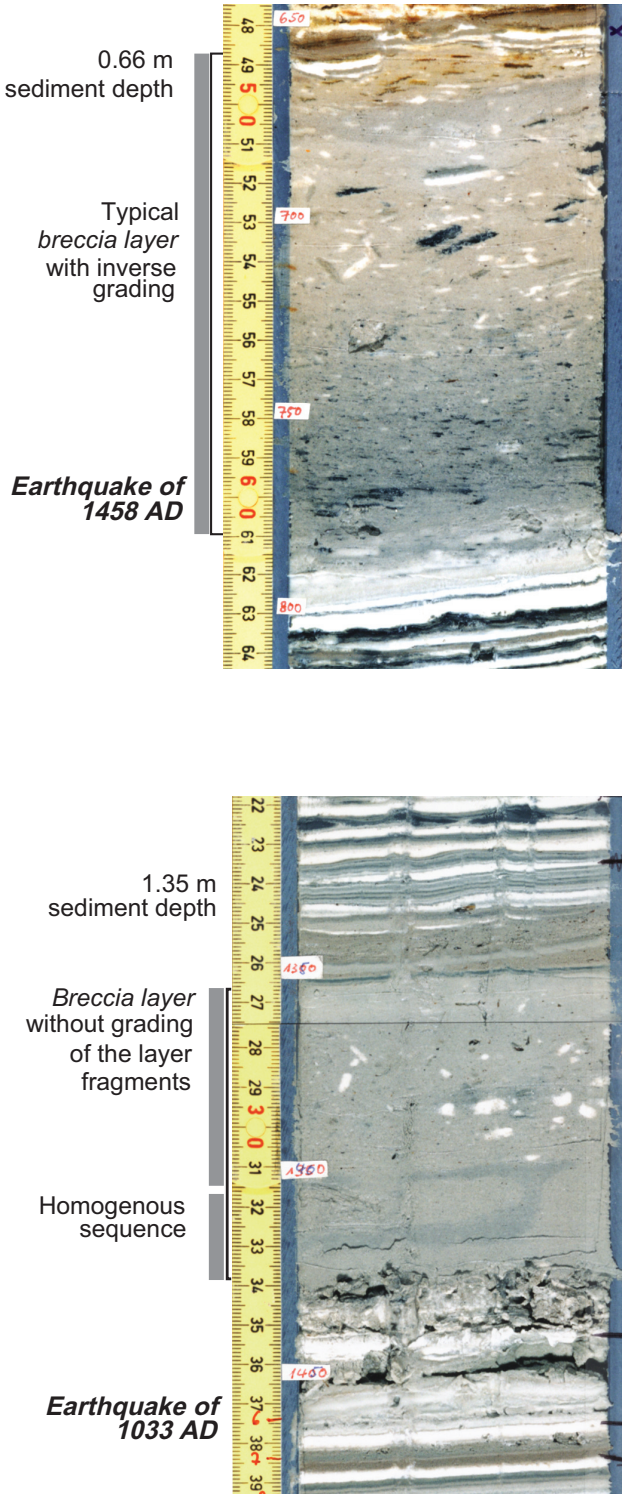

Figure 9. Photos of breccia layers from the Ein Gedi drill core that match the historical earthquakes of 1033 A.D. and 1458 A.D. (Migowski et al., 2004).

region are missing. Clearly, some of these missing historical earthquakes were too distant or too weak to generate significant shaking in Ein Gedi.

While direct historic information on local shaking intensity at Ein Gedi is rare, empirical formulas can evaluate the historic data and estimate the magnitude of a given earthquake, as well as its location (Ambraseys, 1988). In a recent compilation of Middle East intensity data, Ambraseys and Jackson (1998) develop a formula that relates mean earthquake magnitudes to the intensity of shaking at given source distances:

$$M = -1.74 + 0.66\,I + 0.0015\,R + 2.26\,\log R, \qquad (1)$$

where R is the distance from the earthquake focus (assumed at 7.4 km depth), I is the local intensity, and M is the magnitude. Formulas of this form, known as attenuation relations, estimate the local intensity at a site if both the earthquake magnitude and its location are known. A sufficiently close earthquake source with sufficiently large magnitude should generate intraclast breccia layers; sources that are too weak or too distant would not generate intraclast breccia layers. Figure 11 shows a compilation of all historical and instrumental earthquake sources in terms of magnitude and distance from Ein Gedi. The diagonal bold curves separate three domains: strong and close sources on the lower right, all matched with breccia layers; weak and far sources on the upper left, all unmatched; a median domain where about half of the events are matched by intraclast breccia layers. These lines can be fitted to equations of the form of equation (1). The straight line is given by

$$M = 1.9\,\log R + 2.8. \qquad (2)$$

The dotted and dashed lines in Figure 11 mark intensities V and VI, respectively. Note that for distances $R > 50$ km and magnitudes $M > 5.5$, we can consider the isoseismal $I = \mathrm{V}$ as a domain boundary. At lower distances and magnitudes, a higher intensity seems to be required for generating breccia layers.

As shown in Figure 11, all historical earthquakes with calculated local intensity at Ein Gedi $I > \mathrm{V}$ are matched with intraclast breccia. The earthquake of 363 A.D. may constitute an exception to that rule.

The unique match of the two independent records, namely the historical and the one derived from the core, supports three assumptions used to develop the chronological model: (1) breccia layers form by seismic shaking, (2) strong shaking results in breccia layers, and (3) the lamination is seasonal with a detectable annual cycle.

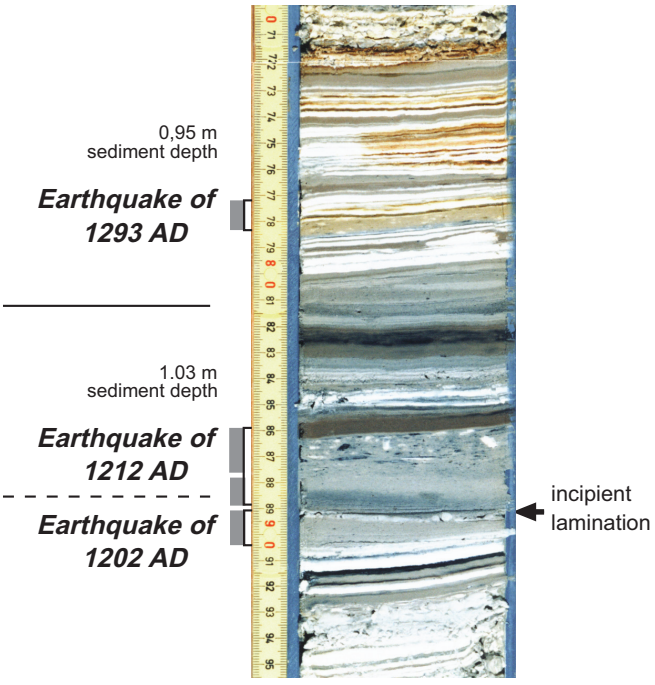

Figure 10. Photo of a section of the Ein Gedi core containing three breccia layers with the respective dates of earthquakes. The 1202 A.D. event is barely determined because the 1212 event almost obliterated the 10-yr-old breccia. Nonetheless, a few laminae (arrow) can be resolved above event horizon 1202 A.D. Migowski et al. (2004) have inferred five unresolved events by correlation of the lamina-counting record of breccia layers with the historical record of destructive earthquakes.

RECURRENCE PATTERNS OF BRECCIA EVENTS

Different paleoseismic and historic studies have indicated different recurrence intervals ranging from a century (Amiran et al., 1994) to ten millennia (Kagan et al., 2005). In some cases, the discrepancy is attributed to the threshold for detection (see Kagan et al., 2005); in others, the discrepancy may arise from the different time window studied (see Ken-Tor et al., 2001a, 2001b). The variation of recurrence interval with time is a manifestation of clustering (Marco et al., 1996b), and it can arise from the complex mechanics of the fault system (Lyakhovsky et al., 2001). Here we consider the influence of the rate of deposition on the resolution of events and discuss the effect of resolution on the apparent recurrence patterns.

Temporal Resolution of the Paleoseismic Record

Sedimentation rate influences the ability to detect individual events in the paleoseismic record. Migowski et al. (2004) discussed the "masking" of an earthquake by a subsequent earthquake as inferred for the Ein Gedi core, and Figure 8 shows possible examples from the Ze'elim outcrop (the pairs of 64–31 B.C. and 1202–1212 A.D.). Figure 10 shows how the breccia layers associated with the 1202 and 1212 A.D. pair are barely resolved from each other in the Ein Gedi core (Migowski et al., 2004).

The temporal resolution (T_{res}) of individual earthquakes in well-stratified lacustrine deposits depends on the rate of sedimentation, R_s, and the thickness of the breccia formed by the subsequent earthquake, H_b. The resolution limit for an

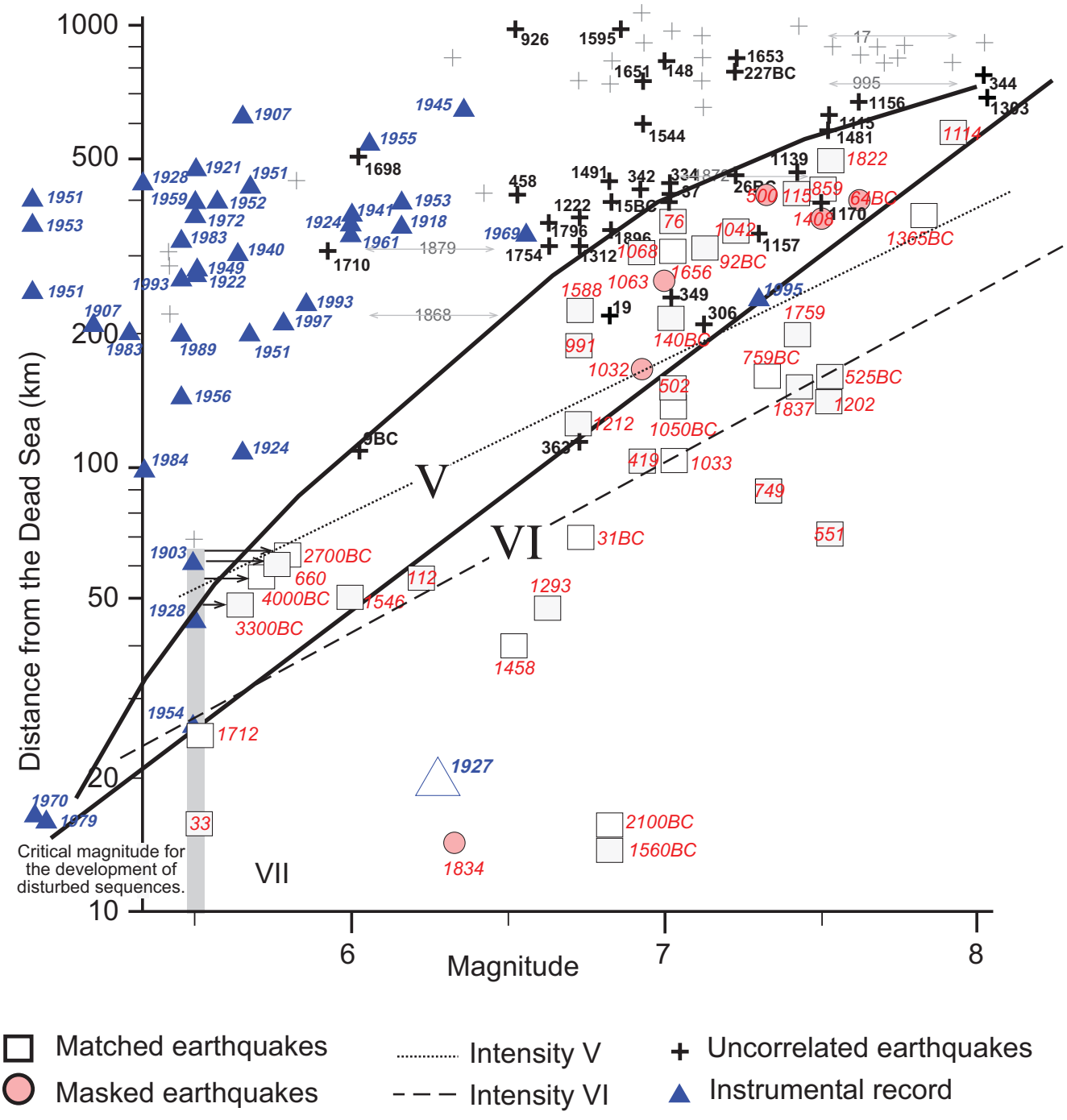

Figure 11. Magnitude-distance field showing all regional and local earthquakes that could affect the Dead Sea. Each marker on the diagram corresponds to a historical or instrumental earthquake recorded in the region. The bold line and the bold curve separate three domains: the lower-right with close and strong earthquakes, all of which represented in the intraclast breccia record; the upper-left with far and weak sources, none of which are represented in the record; and a median domain in which only some earthquakes are recorded by intraclast breccias. The dashed lines correspond to isoseismals. The gray bar represents the threshold magnitude (M = 5.5) for the formation of breccia layers inferred from the diagram. The pattern lends support to the interpretation of the breccia layers as earthquake indicators.

individual earthquake is the critical time interval that can be resolved in a record:

$$T_{res} = H_b/R_s. \quad (3)$$

Equation (3) defines the resolution of a breccia layer with regard to its predecessor based on field observations.

For example, consider the doublet of 1202 and 1212 A.D. earthquakes. In the Ze'elim outcrop, these earthquakes correspond to a single 13-cm-thick breccia layer, whereas in the Ein Gedi core, the events are recorded as two breccia layers, 1.6 and 2.6 cm thick, respectively (Fig. 10, Table 1). The average deposition rate in the Ein Gedi core is about one third of the rate in the Ze'elim section, yet the respective thickness is only one fifth. Indeed, in Ein Gedi we can resolve an intraseismic interval of a decade, whereas in the Ze'elim section, the resolution is three decades. The data for the estimate is given in Table 1. The recurrence interval 1202–1212 A.D. is 10 yr. The deposition rate is given by the thickness of the sediment between the event horizon and the predecessor (or successor) divided by the respective time interval. This definition, applicable only for continuous deposition, neglects possible changes of thickness caused by the breccia formation (redeposition of suspension is likely to fill small-scale bottom topography, some of which may form coseismically).

In the Ein Gedi core, the rate of deposition at the time of the 1212 event is 0.2 cm/yr, and the thickness of the 1212 A.D. breccia is 2.6 cm (Fig. 10). According to Equation (3), T_{res} is thirteen years. This suggests that it is not possible to resolve a decade-long interval between earthquakes, and indeed Migowski et al. (2004) considered the 1202 A.D. event to be "masked." Close inspection of Figure 10 shows that a pair of aragonite-detritus laminae seems to separate the two events, suggesting that the brecciated interval corresponds to 9 yr. If correct, this indicates a deposition rate of ~0.3 cm/yr, slightly higher than the ratio between the breccia thickness and the interseismic interval. Note that all these estimates neglect lateral transport of sediment, yet this assumption is not valid in the presence of local topography. Indeed, Figure 10 indicates that small-scale topography is filled by the laminae postdating 1202 A.D. and by the breccia layer corresponding to 1212 A.D. earthquake.

The breccia layer corresponding to the 1202–1212 A.D. doublet in Ze'elim section has H_b = 13 cm, corresponding to 26 yr of deposition at a rate of 0.5 cm/yr (Fig. 9). The calculated resolution limit is 26 yr, significantly longer than the actual recurrence interval of 10 yr. The subsequent earthquake of 1293 A.D. corresponds to an 18-cm-thick breccia layer (Fig. 9), with a resolution limit of 36 yr, about half the historical recurrence interval. This is why the 1212 and 1293 A.D. earthquakes are resolved in the Ze'elim outcrop.

As we saw for the breccia layer associated with the 1212 A.D. earthquake in the Ein Gedi core, the measured thickness of a breccia layer in the field is only a proxy for the thickness of the sediment that brecciated during an event. Inaccuracies in this proxy may result from differential compaction, suspended sediment in the breccia layer filling local topography, and inclusion of earlier unresolved events. Due to these inaccuracies, we use the mean values of observational data for analyzing resolution in the Lisan Formation.

TABLE 1. HISTORICAL EARTHQUAKES, EIN GEDI CORE AND ZE'ELIM SECTION

Year	ΔT	Ein Gedi R_s = 0.2 cm/yr		Ze'elim R_s = 0.5 cm/yr	
		H_b (cm)	T_{res} (yr)	H_b (cm)	T_{res} (yr)
1293 AD	81	1	5	18	36
1212 AD	10	2.6	13	13	26
1202 AD	88	1.6	8	unresolved	
1114 AD		0.8	4		

Note: Examples of historical earthquakes, interseismic intervals (ΔT), thicknesses of breccia layers (H_b), and deposition rates (R_s) in the Ein Gedi core (data from Migowski et al. [2004]) and Ze'elim section (Ken-Tor et al. [2001a]). We refer to thickness of a breccia layer as an upper bound for the breccia associated with an event horizon as some of the thickness may result from an unresolved preceding event. T_{res}—temporal resolution.

Evidence of Long-Term (>10 k.y.) Clustering

Temporal clustering of earthquakes has been long recognized in the short term covered by instrumental seismicity records (e.g., Ni and Wallace, 1988) and in catalogues of historical seismicity (e.g., Swan, 1988). Mechanical explanations for clustering include interaction between adjacent fault segments with possible evolution of the mechanical properties of the crust (Lyakhovsky et al., 2001; Lynch et al., 2003). The Dead Sea basin is situated between two segments of the transform (Fig. 1) and the long-term sedimentary records can potentially provide data on long-term clustering.

The recognition of intraclast breccias as earthquake indicators is rather new, and more work is required on the influence of local conditions on breccia formation. Yet tentative conclusions on the behavior of the sources for earthquakes can be offered. The main observation afforded by the long paleoseismic records from the Dead Sea basin's lacustrine deposits is that strong earthquakes are clustered over a variety of time scales, at least as long as 10^4 yr (Marco and Agnon, 2005; Marco et al., 1996b; Migowski et al., 2004).

To assess the extent of clustering in interval population, Marco et al. (1996b) used a simple statistic: the standard deviation normalized by the mean (SDN) (also known as the coefficient of variation). For a periodic series with a constant interval (vanishing variance), this ratio vanishes. When the standard deviation is larger than the mean, the population is considered clustered (Kagan and Jackson, 1991).

Marco et al. (1996b) analyzed the temporal distribution of intraclast breccia in three columnar sections of Lisan Formation. In all three sections, the standard deviation of the thickness intervals

exceeded the mean. So, assuming a constant deposition rate, the three sections indicate a temporal clustering of large earthquakes in time. In the PZ1 section, Marco et al. (1996b) went beyond the constant deposition rate approximation: the 36-m-thick section was dated at nine stratigraphic levels using the U-Th method. The age determinations implied a sedimentation-age model with three periods, each with a different rate of sedimentation. More recent field work and additional U-Th ages dating have modified the sedimentation-age model (Haase-Schramm et al., 2004; Stein and Goldstein, this volume). The present sedimentation-age model, based on a total of 22 age determinations, also accounts for a hiatus required by field observations (Machlus et al., 2000). Using the new deposition-age model, the SDN is 1.6, comparing with 1.8 according to the earlier deposition-age model (Table 2). The SDN is not sensitive to the hiatus between 44 and 49 ka or a possible hiatus between 67 and 62 ka (Haase-Schramm et al., 2004). We verified this by calculating statistics for synthetic records in which additional hypothetical earthquakes are introduced in the hiatuses separated by the mean interval.

Calculating the mean and standard deviation of thickness intervals between event horizons amounts to assuming a uniform rate of sedimentation. Doing this, we approximate the SDN of PZ1 at 1.5 (Table 2). If this is the case for the other sections, then SDN ≥ 1, suggesting that all sections have clustered time series. Similar clustering has been reproduced in a mechanical model that accounts for fault network evolution including rupture and healing (Lyakhovsky et al., 2001).

The mean rate of recurrence of intraclast breccia layers inferred from the late Pleistocene Lisan Formation is 2–3 events per five millennia, varying between nine and zero events per five millennia (Fig. 12). The average thickness of breccia layers in PZ1 is 15 cm. The late Pleistocene earthquake clusters show a peak rate of nine events per five millennia, between 50 and 55 ka (Marco et al. 1996b). This recurrence rate corresponds to an average interval of 500–600 yr. Two additional clusters are evident ca. 40 and 20 ka, respectively. The averages of thicknesses of breccia layers formed during the three clusters are 17, 19, and 8 cm, respectively (Table 3). The typical resolution limit for an earthquake is three

TABLE 2. THE STATISTICS OF RECURRENCE OF INTRACLAST BRECCIAS IN LATE QUATERNARY SECTIONS

Stratigraphic section	Mean interval	Record span	No. of events	Standard deviation of intervals	SDN
Time					
PZ1 (late Pleistocene)					
Marco et al. (1996b)	1.6 k.y.	50 k.y.		2.9 k.y.	1.8
Present study	1.9 k.y.	50 k.y.		3.0 k.y.	1.6
Ein Gedi (Holocene)					
historic	50 yr	2 k.y.	32	67 yr	0.75
upper 5 m	98 yr	4 k.y.	41	88 yr	0.9
Thickness					
PZ1	130 cm	50 k.y.		199 cm	1.5
PZ2	109 cm	50 k.y.		123 cm	1.1
M1	101 cm	50 k.y.		100 cm	1.0

Note: The top section of this table (Time) refers to time determinations in sections with well-dated records (the Ein Gedi historic data refers to the period 140 B.C.–1927 A.D.). The bottom section (Thickness) refers to the thickness of intervals between event horizons. SDN—standard deviation normalized by the mean.

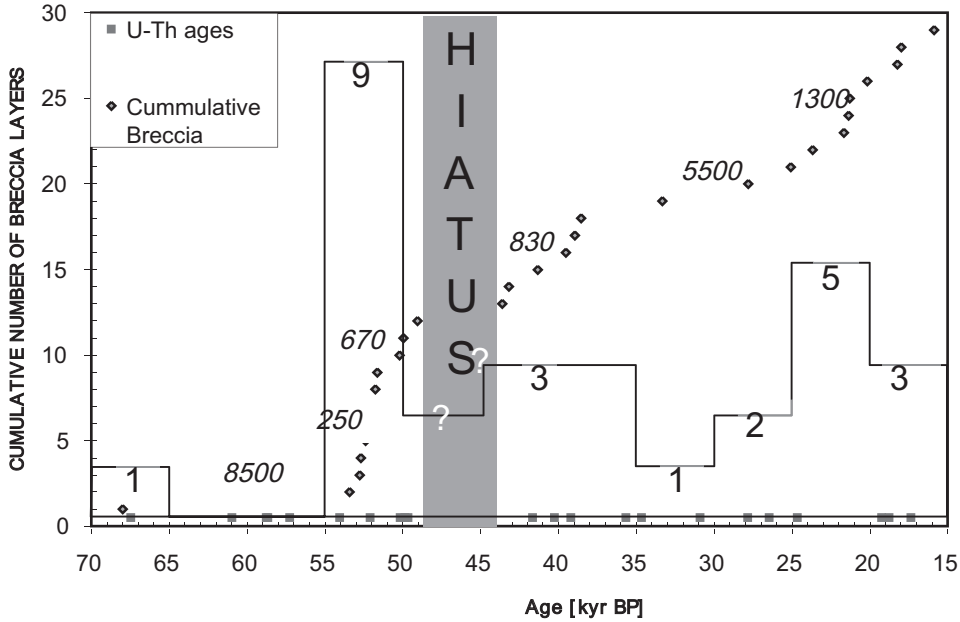

Figure 12. The age estimates of intraclast breccias in the PZ1 section of the Lisan Formation. Measured ages shown as diamonds; inferred seismicity rates are shown as scaled bars with number of events per 5000 yr shown on top of each bar. The numbers in italics denote the recurrence interval in years for segments in the record where the interval seems uniform. The diamonds at the bottom denote the U-Th age determinations of Lisan samples (Haase-Schramm et al., 2004). These age determinations constrain the ages of the seismites by interpolation.

TABLE 3. RESOLUTION OF EARTHQUAKES IN SECTIONS OF LATE PLEISTOCENE PERATZIM CREEK

PZ1	Time span (k.y. B.P.)	H_{dl} (cm)	RI (100 yr)	Mean H_b (cm)	Mean R_s (cm/yr)	T_{res} (100 yr)
All	20–70	2	19	15	0.08	2
1st cluster	51.6–52.8	3	2	17	0.14	1
2nd cluster	38.6–43.6	6	10	19	0.07	3
3rd cluster	18.0–21.7	6	7	8	0.07	1

Note: PZ1—Late Pleistocene Peratzim Creek; earthquake resolution calculated according to Eq. (3) in text. RI—recurrence interval. Columnar section described by Marco et al. (1996b). Dates measured and interpolated by Hasse-Schramm et al., 2004 (see Fig. 12).

hundred years for the second cluster and a hundred years for the other two (two hundred for the entire PZ1 section). This estimate suggests that resolution is not a limiting factor in detecting long-term earthquake clusters in the late Pleistocene lacustrine sections. During the cluster ca. 52 ka, the recurrence rate might exceed the estimate from our data due to lack of resolution.

The recurrence interval for the cluster between 55 and 50 ka is similar to the results of Enzel et al. (2000) from a fan delta in the Dead Sea basin for the past 6 k.y. This is consistent with the suggestion of Enzel et al. (2000), based on a comparison of their mean recurrence interval with that of the entire Lisan Formation, that their late Holocene data represent a cluster of earthquakes.

Another factor that affects the resolution of earthquakes in the lacustrine record is the detection limit of individual breccia layers, H_{dl}. The recognition of a breccia layer depends on the thickness of individual laminae and color contrast between neighboring laminae, which vary from section to section and within sections. Moreover, the method of inspection of the section controls H_{dl}: the detection limit under the microscope is a few millimeters (Fig. 2B), whereas in outcrop it is 2 cm at best. We approximate the detection limit for a given section by the thickness of the thinnest breccia layer, allowing for variations in exposure, color contrasts, and rate of sedimentation.

The variable H_{dl} is useful for the comparison of seismicity recorded by different sections. The recurrence rate in PZ1 peaks ca. 52 ka (Fig. 12) with a recurrence interval of 170 yr. For a similar time span, the recurrence rate inferred for the Ein Gedi core peaks in the past 2 k.y. with a mean recurrence interval of 50 yr (Table 2). The thinnest breccia layer reported in PZ1 is 2 cm, and in the 52 ka cluster it is 3 cm, compared with 2 mm in the Ein Gedi core (Migowski et al., 2004, their Table 2). It is likely that microscopic inspection of the Lisan sediments would reveal additional breccia layers that could not be confidently detected in the field and were classified as clastic layers. Even with such a microscopic study, one would need to account for the threefold ratio between the rates of sedimentation (compare R_s in Tables 1 and 3).

Short-Term (10^2 yr) Recurrence

The normalized standard deviation of the historic section in the Ein Gedi record is 0.75, whereas for the entire section SDN = 0.9 (Table 2). Hence, the statistics do not indicate clustering. Migowski et al. (2004) noted variation in the rate of recurrence in the Dead Sea paleoseismic-historical record, with recurrence rates changing drastically on a time scale of half a millennium. This behavior is reminiscent of the historical record of the Anatolian Faults during the first millennium and half of the second millennium A.D. Ambraseys (1971) has pointed out that the historical record of the North and East Anatolian faults show alternation of activity on a 0.5 k.y. time scale. We further this comparison by seeking intervals of uniform rate of seismicity in all three records. We were able to define uniform rates, such that for each of the Anatolian faults, the rate of seismicity fluctuates between two levels of intervals. Figure 13 reproduces Ambraseys' (1971) representation of the cumulative number of earthquakes versus calendar years in the North and East Anatolian faults together with our data from Dead Sea breccia layers. Figure 13 is striking in two aspects: The first is the uniformity of recurrence rates during several centuries, with rather abrupt shifts. This is clear on the upper panel that shows box-car functions describing the shifting rates in terms of recurrence intervals. The second striking aspect is the timing of the shifts, simultaneous in pairs of faults. At the fifth century A.D., the East Anatolian fault shows an order of magnitude decrease in recurrence interval from 70 yr to 8 yr. At about that time, the recurrence interval of Dead Sea breccia layers decreases from 300 yr to 95 yr. Shortly afterward, the recurrence interval recorded in the North Anatolian fault increases by an order of magnitude from a decade to a century. This quiescent period ends in the tenth century A.D., when the recurrence interval decreases back to a decade. Shortly before the end of the tenth century, the recurrence interval inferred from the Dead Sea breccias decreases from 95 to 50 yr. The recurrence interval increases back to a medium level of 74 yr at the fourteenth century A.D., simultaneously with the order of magnitude increase in the East Anatolian Fault that returns to a recurrence interval of 70 yr.

It is tempting to draw conclusions from these records on the behavior of the plate boundaries. One should keep in mind that these records may be biased as they record ground shaking on the site of the recorder (Dead Sea sediments or Old World chroniclers). Even so the periods of frequent activity are reminiscent of the twentieth century in the North Anatolian Fault, where a series of ruptures have propagated along the plate boundary from east to

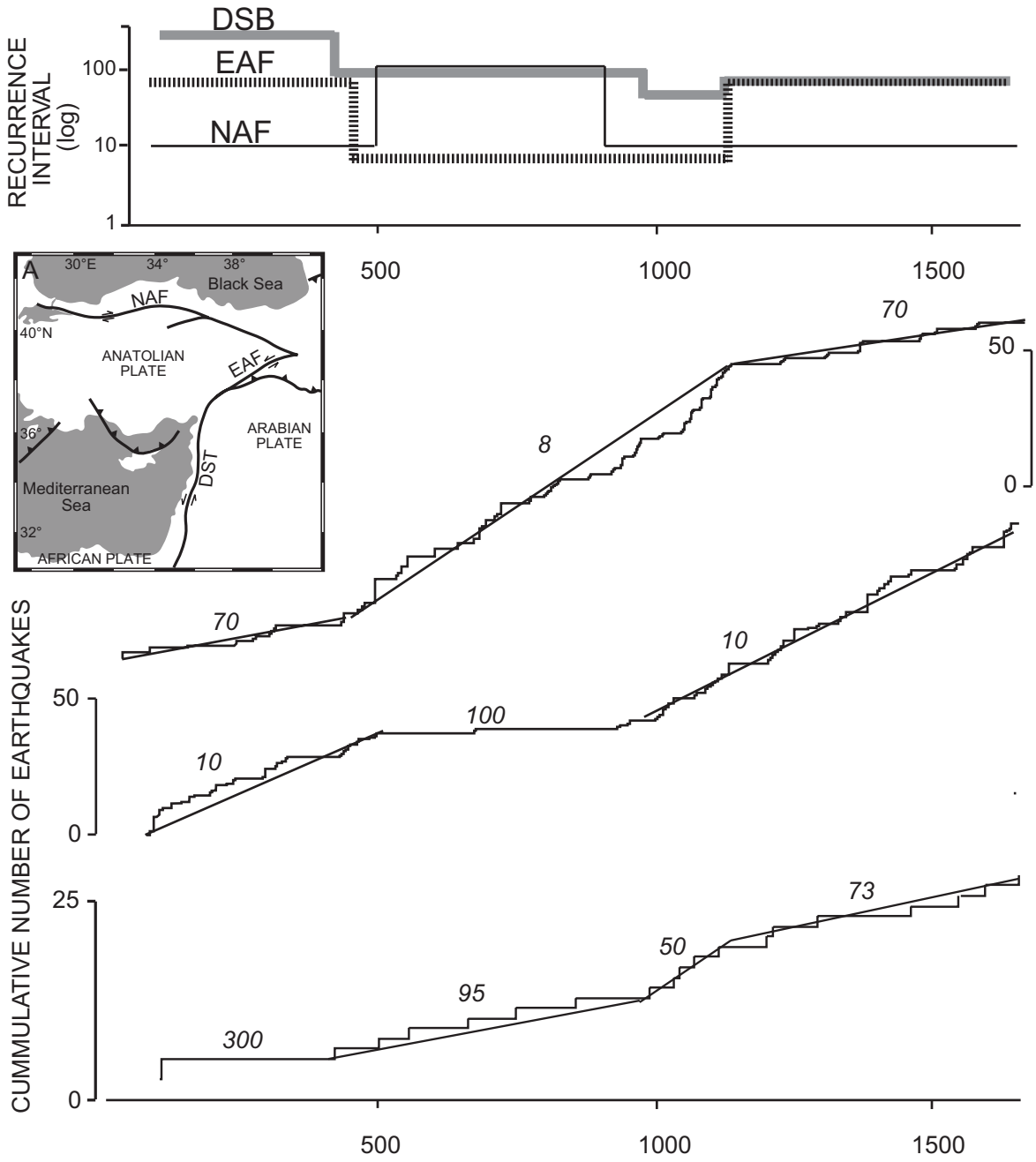

Figure 13. Cumulative seismicity along three plate boundaries. Top: Recurrence intervals as a function of time for three plate boundaries. DSB is the record from the Dead Sea Basin. The values are estimated based on the bottom panel. Center (A): The plate configuration with the North Anatolian fault (NAF) bounding the Anatolia plate from north and north east, where it meets the East Anatolian fault (EAF). The latter is fed from the south by the Dead Sea transform (DST) fault. Bottom: Cumulative number of earthquakes in the historical records of Anatolian faults according to Ambraseys (1971) (right hand coordinate) and the record of breccias from the DSB (left hand coordinate, expanded)

west (Toksoz et al., 1979; Stein et al., 1997b). Similarly, the series of earthquakes recorded in the Dead Sea from the beginning of the second millennium A.D. seems to follow a similar propagation pattern from north to south (Marco and Agnon, 2000, 2005). If the record indeed indicates shifts in activity along the plate boundary, the concerted transitions may indicate a mechanical coupling.

CONCLUSIONS

The systematic approach to accumulating observations on intraclast breccia layers permits their analysis as recorders of paleo-earthquakes. Such breccia layers, previously called "mixed layers," are abundant in sedimentary sections of Quaternary lakes from the Dead Sea basin. The finding of intraclast breccia layers juxtaposed against surface faults has driven a wide range of studies focused on these long-term seismic recorders. The fault scarps form a fault zone, traced to the subsurface by high-resolution geophysical surveys. This fault zone is a subsidiary structure to the master fault bounding the Dead Sea basin from the west and extending north to the transform plate boundary. While the record of displacement of the fault zone is limited to particular slip events that activate this secondary structure, the record of breccia layers may be complete for events that rupture the plate boundary.

We define field criteria for the identification of intraclast breccias, focusing on features that can indicate a seismic origin. The wealth of data for such earthquake indicators collected in natural outcrops within the Dead Sea basin offers insights into the phenomenology and systematics of earthquakes on time scales that are not obtainable elsewhere.

Cores from the receding shore of the Dead Sea contain continuous sedimentary records of the past 10 k.y., undisturbed by lowstands. The Ein Gedi core features 3 m of alternating seasonal laminae. The two independent earthquake records—historical and sedimentary—offer a simultaneous test regarding two hypotheses: the earthquake origin of breccia and the annual cycle of laminae. The likelihood of matching historical earthquakes with an arbitrary time series that corresponds to the breccia layers in the core is negligible. The observation that the breccia layers match earthquakes from the historical catalogues that are strong and/or close to the coring site supports both hypotheses (Fig. 11). Changes in the rate of recurrence of earthquakes in the Dead Sea record during the historical period seem to correlate with changes in the Anatolian Fault system. If the rates of recurrence could be taken as indicators of activity of the plate boundaries, then these plate boundaries might be coupled on the time scale of 500 yr.

The brecciation from an earthquake that succeeds another strong earthquake might obliterate the breccia layer of the predecessor. This hampers the potential that lies in the laminated sediment to resolve pairs of earthquakes. The resolution of an interseismic interval is no better than the ratio of the thickness of a breccia layer to the rate of deposition. But the resolution limit of individual earthquakes does not affect the observation of clustering in the record, which is evident in the long periods of quiescence alternating with periods of recurrence of earthquakes. During most of the period recorded, we find that the apparent recurrence interval is significantly longer than the resolution limit. During a cluster of earthquakes ca. 52 ka, the interseismic interval becomes shorter than 200 yr, which is close to the resolution limit for the Lisan outcrops.

ACKNOWLEDGMENTS

This paper summarizes over a decade of research during which many individuals have contributed significantly to our understanding of the phenomena of seismogenic breccia layers. Z. Reches introduced us to the potential of the Lisan Formation as a recorder of earthquake deformations. M. Stein supported this research by providing dates. Y. Enzel prompted us to formulate our assumptions better. J. Negendank has contributed from his invaluable experience working with cores. We wish to thank these and the following researchers for useful discussions: A. Katz, Y. Kolodny, Z. Garfunkel, Y. Hamiel, R. Weinberger, K. Hsu, A. Nur, M. McWilliams, and Y. Bartov. A. Crone, Y. Eyal, and T. Rockwell provided useful reviews. E. Kagan provided essential help with the revised manuscript. E. Ram provided field assistance. The research was supported by the German-Israel Binational Science Foundation (GIF) and by the Israel Science Foundation and the Israel-USA Binational Science Foundation.

REFERENCES CITED

Agnon, A., 1982, Post Lisan faulting at the Dead Sea graben border: Jerusalem, Israel Geological Society Annual Meeting, Elat, p. 1–2.

Agnon, A., 1983, The evolution of sedimentary basins and the morphotectonics in the western fault escarpment of the Dead Sea [M.Sc. thesis]: Jerusalem, Hebrew University, 61 p.

Allen, C.R., 1974, Geological criteria for evaluating seismicity: Geological Society of America Bulletin, v. 86, p. 1041–1057, doi: 10.1130/0016-7606(1975)86<1041:GCFES>2.0.CO;2.

Allen, J.R.L., 1982, Sedimentary structures: Their character and physical basis: Developments in sedimentology: New York, Elsevier, 663 p.

Ambraseys, N.N., 1971, Value of historical records of earthquakes: Nature, v. 232, no. 5310, p. 375–379, doi: 10.1038/232375a0.

Ambraseys, N.N., 1988, Magnitude-fault length relationships for earthquakes in the Middle East, *in* Lee, W.K.H., Meyers, H., and Shimazaki, K., eds., Historical seismograms and earthquakes of the world: San Diego, Academic Press, p. 309–310.

Ambraseys, N.N., and Jackson, J.A., 1998, Faulting associated with historical and recent earthquakes in the eastern Mediterranean region: Geophysical Journal International, v. 133, p. 390–406, doi: 10.1046/j.1365-246X.1998.00508.x.

Ambraseys, N.N., Melville, C.P., and Adams, R.D., 1994, The seismicity of Egypt, Arabia, and the Red Sea: A historical review: Cambridge, Cambridge University Press, 181 p.

Amiran, D.H.K., Arieh, E., and Turcotte, T., 1994, Earthquakes in Israel and adjacent areas: Macroseismic observations since 100 B.C.E: Israel Exploration Journal, v. 44, p. 260–305.

Amit, R., Zilberman, E., Enzel, Y., and Porat, N., 2002, Paleoseismic evidence for time dependency of seismic response on a fault system in the southern Arava valley, Dead Sea rift, Israel: Geological Society of America Bulletin, v. 114, p. 192–206, doi: 10.1130/0016-7606(2002)114<0192:PEFTDO>2.0.CO;2.

Avni, Y., Bartov, Y., Garfunkel, Z., and Ginat, H., 2000, Evolution of the Paran drainage basin and its relation to the Plio-Pleistocene history of the Arava Rift western margin, Israel: Israel Journal of Earth Sciences, v. 49, no. 4, p. 215–238, doi: 10.1560/W8WL-JU3Y-KM7W-8LX4.

Bachrach, R., Nur, A., and Agnon, A., 2001, Liquefaction and dynamic poroelasticity in soft sediments: Journal of Geophysical Research, v. 106, no. B7, p. 13,515–13,526, doi: 10.1029/2000JB900474.

Bartov, Y., 1999, The geology of the Lisan Formation in Masada Plain and the Lisan Peninsula [M.Sc. thesis]: Jerusalem, Hebrew University, 63 p.

Bartov, Y., Stein, M., Enzel, Y., Agnon, A., and Reches, Z., 2002, Lake levels and sequence stratigraphy of Lake Lisan, the late Pleistocene precursor of the Dead Sea: Quaternary Research, v. 57, p. 9–21, doi: 10.1006/qres.2001.2284.

Begin, B.Z., Steinberg, D.M., Ichinose, G.A., and Marco, S., 2005, A 40,000 year unchanging seismic regime in the Dead Sea rift: Geology, v. 33, no. 4, p. 257–260, doi: 10.1130/G21115.1.

Bookman, R. (Ken Tor), Enzel, Y., Agnon, A., and Stein, M., 2004, Late Holocene lake levels of the Dead Sea: Geological Society of America Bulletin, v. 116, p. 555–571, doi: 10.1130/B25286.1.

Bowman, D., 1995, Active surface ruptures on the northern Arava Fault, the Dead Sea Rift: Israel Journal of Earth Sciences, v. 44, no. 1, p. 51–59.

Bowman, D., Banet-Davidovich, D., Bruins-Hendrik, J., and van der Plicht, J., 2000, Dead Sea shoreline facies with seismically-induced soft-sediment deformation structures, Israel: Israel Journal of Earth Sciences, v. 49, no. 4, p. 197–214, doi: 10.1560/GXHT-AK5W-46EF-VTR8.

Chapron, E., Beck, C., Pourchet, M., and Deconinck, J.F., 1999, 1822 earthquake-triggered homogenite in Lake Le Bourget (NW Alps): Terra Nova, v. 11, no. 2–3, p. 86–92, doi: 10.1046/j.1365-3121.1999.00230.x.

Cita, M.B., Camerlenghi, A., and Rimoldi, B., 1996, Deep-sea tsunami deposits in the eastern Mediterranean: New evidence and depositional models: Sedimentary Geology, v. 104, no. 1–4, p. 155–173, doi: 10.1016/0037-0738(95)00126-3.

Davenport, C.A., and Ringrose, P.S., 1987, Deformation of Scottish Quaternary sediment sequence by strong earthquake motions, *in* Jones, M.E., and Preston, R.M., eds., Deformation of sediments and sedimentary rocks: London, Geological Society Special Publication 29, p. 299–314.

Doig, R., 1990, 2300 yr history of seismicity from silting events in Lake Tadoussac, Chrlevoix, Quebec: Geology, v. 18, p. 820–823, doi: 10.1130/0091-7613(1990)018<0820:YHOSFS>2.3.CO;2.

Doig, R., 1991, Effects of strong seismic shaking in lake sediments, and earthquake recurrence interval, Témiscaming, Quebec: Canadian Journal of Earth Sciences, v. 28, no. 9, p. 1349–1352.

El-Isa, Z.H., and Mustafa, H., 1986, Earthquake deformations in the Lisan deposits and seismotectonic implications: Geophysical Journal, Royal Astronomical Society, v. 86, p. 413–424.

Ellenblum, R., Marco, S., Agnon, A., Rockwell, T., and Boas, A., 1998, Crusader castle torn apart by earthquake at dawn, 20 May 1202: Geology, v. 26, no. 4, p. 303–306, doi: 10.1130/0091-7613(1998)026<0303:CCTABE>2.3.CO;2.

Enzel, Y., Kadan, G., and Eyal, Y., 2000, Holocene earthquakes inferred from a fan-delta sequence in the Dead Sea graben: Quaternary Research, v. 53, no. 1, p. 34–48, doi: 10.1006/qres.1999.2096.

Eyal, Y., Bruner, I., Cadan, G., Enzel, Y., and Landa, E., 2002, High-resolution seismic study of the Nahal Darga fan delta, Dead Sea Israel, with the aim to relate the surface and subsurface tectonic structures: European Geophysical Union Stephan Muller Special Publication Series, v. 2, p. 21–33.

Freund, R., 1965, A model of the structural development of Israel and adjacent areas since Upper Cretaceous times: Geological Magazine, v. 102, p. 189–205.

Gardosh, M., Reches, Z., and Garfunkel, Z., 1990, Holocene tectonic deformation along the western margins of the Dead Sea: Tectonophysics, v. 180, p. 123–137, doi: 10.1016/0040-1951(90)90377-K.

Garfunkel, Z., 1981, Internal structure of the Dead Sea leaky transform (rift) in relation to plate kinematics: Tectonophysics, v. 80, p. 81–108, doi: 10.1016/0040-1951(81)90143-8.

Garfunkel, Z., Zak, I., and Freund, R., 1981, Active faulting in the Dead Sea rift: Tectonophysics, v. 80, p. 1–26, doi: 10.1016/0040-1951(81)90139-6.

Gluck, D., 2001, The landscape evolution of the southwestern Dead Sea basin and the paleoseismic record of the southwestern marginal fault of the Dead Sea basin and the Carmel fault during the late Pleistocene and the Holocene [M.Sc. thesis]: Jerusalem, Hebrew University, 86 p.

Guidoboni, E., 1994, Catalogue of ancient earthquakes in the Mediterranean area up to the 10th century: Rome, Istituto Nazionale di Geofisica, 504 p.

Haase-Schramm, A., Goldstein, S.L., and Stein, M., 2004, U-Th dating of Lake Lisan (late Pleistocene Dead Sea) aragonite and implications for glacial East Mediterranean climate change: Geochimica et Cosmochimica Acta, v. 68, no. 5, p. 985–1005, doi: 10.1016/j.gca.2003.07.016.

Hamiel, Y., 1999, Dynamic behavior under vibration: Laboratory experiments with sediments, wave propagation in non-linear elastic medium and possible implications to earthquakes [M.Sc. thesis]: Jerusalem, Hebrew University, 63 p.

Hatanaka, M., Uchida, A., and Ohara, J., 1997, Liquefaction characteristics of a gravelly fill liquefied during the 1995 Hyogo-Ken Nanbu earthquake: Soils and Foundations, v. 37, no. 3, p. 107–115.

Heifetz, E., Agnon, A., and Marco, S., 2005, Soft sediment deformation by Kelvin Helmholtz Instability: A case from Dead Sea earthquakes: Earth and Planetary Science Letters, v. 236 p. 497–504.

Hofstetter, A., Thio, H.K., and Shamir, G., 2003, Source mechanism of the 22/11/1995 Gulf of Aqaba earthquake and its aftershock sequence: Journal of Seismology, v. 7, p. 99–114, doi: 10.1023/A:1021206930730.

Jackson, J.A., and Bates, R.L., 1997, Glossary of Geology: Alexandria, Virginia, American Geological Institute, 769 p.

Jones, A.P., and Omoto, K., 2000, Towards establishing criteria for identifying trigger mechanisms for soft-sediment deformation: A case study of Late Pleistocene lacustrine sands and clays, Onikobe and Nakayamadaira Basins, northeastern Japan: Sedimentology, v. 47, no. 6, p. 1211–1226, doi: 10.1046/j.1365-3091.2000.00355.x.

Kagan, Y.Y., and Jackson, D.D., 1991, Long-term earthquake clustering: Geophysical Journal International, v. 104, no. 1, p. 117–133.

Kagan, E.J., Agnon, A., Bar-Matthews, M., and Ayalon, A., 2005, Dating large infrequent earthquakes by damaged cave deposits: Geology, v. 33, p. 261–264, doi: 10.1130/G21193.1.

Kahle, C.F., 2002, Seismogenic deformation structures in microbialites and mudstones, Silurian Lockport Dolomite, northwestern Ohio, USA: Journal of Sedimentary Research, v. 72, p. 201–216.

Kanasewich, E., and Phadke, S., 1988, Imaging discontinuities on seismic sections: Geophysics, v. 53, p. 334–345, doi: 10.1190/1.1442467.

Kastens, K.A., and Cita, M.B., 1981, Tsunami-induced sediment transport in the abyssal Mediterranean Sea: Geological Society of America Bulletin, v. 92, p. 845–857, doi: 10.1130/0016-7606(1981)92<845:TSTITA>2.0.CO;2.

Katz, A., Kolodny, Y., and Nissenbaum, A., 1977, The geochemical evolution of the Pleistocene Lake Lisan–Dead Sea system: Geochimica et Cosmochimica Acta, v. 41, p. 1609–1626, doi: 10.1016/0016-7037(77)90172-7.

Ken-Tor, R., Agnon, A., Enzel, Y., Marco, S., Negendank, J.F.W., and Stein, M., 2001a, High-resolution geological record of historic earthquakes in the Dead Sea basin: Journal of Geophysical Research, v. 106, no. B2, p. 2221–2234, doi: 10.1029/2000JB900313.

Ken-Tor, R., Stein, M., Enzel, Y., Agnon, A., Marco, S., and Negendank, J.F.W., 2001b, Precision of calibrated radiocarbon ages of historic earthquakes in the Dead Sea Basin: Radiocarbon, v. 43, no. 3, p. 1371–1382.

Kitamura, A., Tominaga, E., and Sakai, H., 2002, Subaqueous sand blow deposits induced by the 1995 Hyogo-ken Nanbu Earthquake, Japan: Island Arcs, v. 11, no. 1, p. 1–9.

Klinger, Y., Avouac, J.P., Abou-Karaki, N., Dorbath, L., Bourles, D., and Reyss, J.L., 2000, Slip rate on the Dead Sea transform fault in northern Araba Valley (Jordan): Geophysical Journal International, v. 142, p. 755–768, doi: 10.1046/j.1365-246x.2000.00165.x.

Kolodny, Y., Chaussidon, M., and Katz, A., 2005, Geochemistry of a chert breccia: Geochimica et Cosmochimica Acta, v. 69, no. 2, p. 427–439, doi: 10.1016/j.gca.2004.07.010.

Landa, E., Shtivelman, V., and Gelchinsky, V., 1987, A method for detection of diffracted waves on common offset sections: Geophysical Prospecting, v. 35, p. 359–374.

Li, Y., Craven, J., and Schweig, E.S., 1996, Sand boils induced by the 1993 Mississippi River flood: Could they one day be misinterpreted as earthquake-induced liquefaction?: Geology, v. 24, p. 171–174, doi: 10.1130/0091-7613(1996)024<0171:SBIBTM>2.3.CO;2.

Lin, A.M., 1997, Instantaneous-shaking liquefaction induced by the M7.2 1995 Southern Hyogo Prefecture earthquake, Japan: Geology, v. 25, no. 5, p. 435–438, doi: 10.1130/0091-7613(1997)025<0435:ISLIBT>2.3.CO;2.

Lioubashevski, O., Arbell, H., and Fineberg, J., 1996, Dissipative solitary states in driven surface waves: Physical Review Letters, v. 76, no. 21, p. 3959–3962, doi: 10.1103/PhysRevLett.76.3959.

Lyakhovsky, V., Ben-Zion, Y., and Agnon, A., 2001, Fault evolution and seismicity patterns in a rheologically layered halfspace: Journal of Geophysical Research, v. 106, no. B3, p. 4103–4120, doi: 10.1029/2000JB900218.

Lynch, J.C., Burgmann, R., Richards, M.A., and Ferencz, R.M., 2003, When faults communicate: Viscoelastic coupling and earthquake clustering in a simple two-fault system: Geophysical Research Letters, v. 30, no. 6, 1270.

Machlus, M., Enzel, Y., Goldstein, S.L., Marco, S., and Stein, M., 2000, Reconstruction of low-stands of Lake Lisan between 55 and 35 kyr: Quaternary International, v. 73-74, p. 137–144, doi: 10.1016/S1040-6182(00)00070-7.

Marco, S., and Agnon, A., 1995, Prehistoric earthquake deformations near Masada, Dead Sea graben: Geology, v. 23, no. 8, p. 695–698, doi: 10.1130/0091-7613(1995)023<0695:PEDNMD>2.3.CO;2.

Marco, S., and Agnon, A., 2000, Patterns of earthquake recurrence: Initial results from the Dead Sea Transform, *in* Israel Geological Society Annual Meeting Meeting, Ma'alot, p. 84.

Marco, S., and Agnon, A., 2005, Repeated earthquake faulting revealed by high-resolution stratigraphy: Tectonophysics, v. 401, p. 101–112.

Marco, S., Agnon, A., Bruner, I., Landa, E., and Ron, H., 1996a, The Masada fault zone (Dead Sea Graben) in outcrop and geophysical images: Institute for Petroleum Research and Geophysics, P54/180/95.

Marco, S., Stein, M., Agnon, A., and Ron, H., 1996b, Long term earthquake clustering: A 50,000 year paleoseismic record in the Dead Sea Graben: Journal of Geophysical Research, v. 101, no. B3, p. 6179–6192, doi: 10.1029/95JB01587.

Marco, S., Rockwell, T.K., Agnon, A., Heimann, A., and Frieslander, U., 2005, Late Holocene slip of the Dead Sea Transform revealed in 3D palaeoseismic trenches on the Jordan Gorge Fault: Earth and Planetary Science Letters, v. 234, no. 1–2, p. 189–205, doi: 10.1016/j.epsl.2005.01.017.

McCalpin, J.P., 1996, Paleoseismology, *in* Dmowska, R., and Holton, J.R., eds., International Geophysical Series: San Diego, Academic Press, v. 62, p. 588.

Meghraoui, M., Gomez, F., Sbeinati, R., derWoerd, J.V., Mouty, M., Darkal, A.N., Radwan, Y., Layyous, I., Najjar, H.A., Darawcheh, R., Hijazi, F., Al-Ghazzi, R., and Barazangi, M., 2003, Evidence for 830 years of seismic quiescence from palaeoseismology, archaeoseismology and historical seismicity along the Dead Sea fault in Syria: Earth and Planetary Science Letters, v. 210, p. 35–52, doi: 10.1016/S0012–821X(03)00144–4.

Migowski, C., Agnon, A., Bookman, R., Negendank, J.F.W., and Stein, M., 2004, Recurrence pattern of Holocene earthquakes along the Dead Sea transform revealed by varve-counting and radiocarbon dating of lacustrine sediments: Earth and Planetary Science Letters, v. 222, p. 301–314, doi: 10.1016/j.epsl.2004.02.015.

Neev, D., and Emery, K.O., 1967, The Dead Sea, depositional processes and environments of evaporites: Geological Survey of Israel Bulletin, v. 41, p. 147.

Ni, J., and Wallace, T., 1988, Temporal clustering of earthquakes; examples from the Basin and Range Province: Seismological Research Letters, v. 59, no. 4, p. 316–327.

Niemi, T.M., and Ben-Avraham, Z., 1994, Evidence for Jericho earthquakes from slumped sediments of the Jordan River delta in the Dead Sea: Geology, v. 22, p. 395–398, doi: 10.1130/0091-7613(1994)022<0395:EFJEFS>2.3.CO;2.

Niemi, T.M., Zhang, H., Atallah, M., and Harrison, B.J., 2001, Late Pleistocene and Holocene slip rate of the Northern Wadi Araba fault, Dead Sea Transform, Jordan: Journal of Seismology, v. 5, p. 449–474, doi: 10.1023/A:1011487912054.

Obermeier, S.F., 1996, Use of liquefaction-induced features for paleoseismic analysis: Engineering Geology, v. 44, p. 1–76.

Pettijohn, F.J., Potter, P.E., and Siever, R., 1987, Sand and sandstone: New York, Springer-Verlag, 553 p.

Quennell, A.M., 1956, Tectonics of the Dead Sea rift, *in* Congreso Geológico Internacional, 20th session: Mexico City, Asociación de Servicios Geológicos Africanos, p. 385–405.

Reches, Z., and Hoexter, D.F., 1981, Holocene seismic and tectonic activity in the Dead Sea area: Tectonophysics, v. 80, p. 235–254, doi: 10.1016/0040-1951(81)90151-7.

Rodríguez-Pascua, M.A., De-Vicente, G., Calvo, J.P., and Pérez-López, R., 2003, Similarities between recent seismic activity and paleoseismites during the late Miocene in the external Betic Chain (Spain): Relationship by 'b' value and the fractal dimension: Journal of Structural Geology, v. 25, no. 5, p. 749–763, doi: 10.1016/S0191-8141(02)00078-0.

Sagy, A., Reches, Z., and Agnon, A., 2003, Hierarchic three-dimensional structure and slip partitioning in the western Dead Sea pull-apart: Tectonics, v. 22, no. 1, 1004, doi: 10.1029/2001TC001323.

Siegenthaler, C., Finger, W., Kelts, K., and Wang, S., 1987, Earthquake and seiche deposits in Lake Lucerne, Switzerland: Eclogae Geologicae Helvetica, v. 80, no. 1, p. 241–260.

Seilacher, A., 1969, Fault-graded beds interpreted as seismites: Sedimentology, v. 13, p. 155–159.

Sims, J.D., 1973, Earthquake-induced structures in sediments of the Van Norman Lake, California: Science, v. 1–2, p. 161–163.

Stein, M., Starinsky, A., Katz, A., Goldstein, S., Machlus, M., and Schramm, A., 1997a, Strontium isotopic, chemical, and sedimentological evidence for the evolution of Lake Lisan and the Dead Sea: Geochimica et Cosmochimica Acta, v. 61, no. 18, p. 3975–3992, doi: 10.1016/S0016-7037(97)00191-9.

Stein, R.S., Barka, A., and Dietrich, J.H., 1997b, Progressive failure on the North Anatolian fault since 1939 by earthquake stress triggering: Geophysical Journal International, v. 128, p. 594–604.

Swan, F.H., 1988, Temporal clustering of paleoseismic events on the Oued Fodda fault, Algeria: Geology, v. 16, p. 1092–1095, doi: 10.1130/0091-7613(1988)016<1092:TCOPEO>2.3.CO;2.

Toksoz, M.N., Shakal, A.F., and Michael A.J., 1978, Space-time migration of earthquakes along the North Anatolian Fault Zone and seismic gaps: Pure and Applied Geophysics, v. 117, p. 1258–1270

Wilson, J.T., 1965, A new class of faults and their bearing on continental drift: Nature, no. 4995, p. 343–347.

Yeats, R.S., Sieh, K., and Allen, C.R., 1997, The geology of earthquakes: Oxford, UK, Oxford University Press, 576 p.

Zak, I., and Freund, R.R., 1966, Recent strike-slip movements along the Dead Sea rift: Israel Journal of Earth Sciences, v. 15, p. 33–37.

Manuscript Accepted by the Society 26 July 2005